


## Article

# Effects of Para-Toluenesulfonamide on Canine Melanoma Xenotransplants in a BALB/c Nude Mouse Model

Chien-Teng Lin <sup>1,2</sup>, Chuen-Fu Lin <sup>3</sup>, Jui-Te Wu <sup>2</sup>, Hsiao-Pei Tsai <sup>1,2</sup>, Shu-Ying Cheng <sup>2,4</sup>, Huei-Jyuan Liao <sup>2</sup>, Tzu-Chun Lin <sup>2</sup>, Chao-Hsuan Wu <sup>2,4</sup>, Yu-Chin Lin <sup>2,4</sup>, Jiann-Hsiung Wang <sup>2,\*</sup> and Geng-Ruei Chang <sup>2,\*</sup> 

<sup>1</sup> Ph.D. Program of Agriculture Science, National Chiayi University, 300 University Road, Chiayi 60004, Taiwan

<sup>2</sup> Department of Veterinary Medicine, National Chiayi University, 580 Xinmin Road, Chiayi 60054, Taiwan

<sup>3</sup> Department of Veterinary Medicine, College of Veterinary Medicine, National Pingtung University of Science and Technology, 1 Shuefu Road, Neipu, Pingtung 912301, Taiwan

<sup>4</sup> Department of Pet Medicine, Gongwin Biopharma Co., Ltd., 1 Section, 80 Jianguo North Road, Zhongshan District, Taipei 104001, Taiwan

\* Correspondence: jhwang@mail.ncyu.edu.tw (J.-H.W.); grchang@mail.ncyu.edu.tw (G.-R.C.); Tel.: +886-5-2732959 (J.-H.W.); +886-5-2732946 (G.-R.C.)

**Simple Summary:** Canine melanomas are malignant neoplasms, and primary melanomas arise at the footpad, nail bed, gastrointestinal tract, mucocutaneous junction, and eyes. Para-toluenesulfonamide (PTS) is a small molecule that acts against several cancers (hepatocellular carcinoma, nonsmall-cell lung cancer, and tongue squamous cell carcinoma). The pharmacological pathway of PTS has the potential to exert anti-inflammatory and antithrombotic functions. We established canine melanoma xenografts in mice and randomized the animals into four treatment groups: saline, cisplatin, PTS, and PTS combined with cisplatin. The findings indicated that compared with the control mice, mice treated with PTS and the combination of PTS and cisplatin showed retarded tumor growth; increased tumor apoptosis through the upregulation of caspase 3 and extracellular signal-regulated kinase phosphorylation; decreased inflammation levels of cytokines, such as interleukin-1 $\beta$ , tumor necrosis factor- $\alpha$ , and interleukin-6; reduced inflammation-related factors, such as the cyclooxygenase-2 protein and nuclear factor- $\kappa$ B mRNA; enhanced anti-inflammation-related factors; and inhibition of the metastasis-related factors transforming growth factor  $\beta$ , CD44, epidermal growth factor receptor, and vascular endothelial growth factor. Combining cisplatin with PTS has a stronger effect than PTS alone. These findings may prove useful in further explorations of the application of PTS or PTS combined with cisplatin to the treatment of canine melanoma in general.

**Abstract:** The pharmacological pathway of para-toluenesulfonamide (PTS) restricts the kinase activity of the mammalian target of rapamycin, potentially leading to reductions in cell division, cell growth, cell proliferation, and inflammation. These pathways have a critical effect on tumorigenesis. We aimed to examine the antitumor effect of PTS or PTS combined with cisplatin on canine melanoma implanted in BALB/c nude mice by estimating tumor growth, apoptosis expression, inflammation, and metastasis. The mice were randomly divided into four groups: control, cisplatin, PTS, and PTS combined with cisplatin. Mice treated with PTS or PTS combined with cisplatin had retarded tumor growth and increased tumor apoptosis through the enhanced expression of cleaved caspase 3 and extracellular signal-regulated kinase phosphorylation, decreased inflammatory cytokine levels, reduced inflammation-related factors, enhanced anti-inflammation-related factors, and inhibition of metastasis-related factors. Mice treated with PTS combined with cisplatin exhibited significantly retarded tumor growth, reduced tumor size, and increased tumor inhibition compared with those treated with cisplatin or PTS alone. PTS or PTS combined with cisplatin could retard canine melanoma growth and inhibit tumorigenesis. PTS and cisplatin were found to have an obvious synergistic tumor-inhibiting effect on canine melanoma. PTS alone and PTS combined with cisplatin may be antitumor agents for canine melanoma treatment.



**Citation:** Lin, C.-T.; Lin, C.-F.; Wu, J.-T.; Tsai, H.-P.; Cheng, S.-Y.; Liao, H.-J.; Lin, T.-C.; Wu, C.-H.; Lin, Y.-C.; Wang, J.-H.; et al. Effects of Para-Toluenesulfonamide on Canine Melanoma Xenotransplants in a BALB/c Nude Mouse Model. *Animals* **2022**, *12*, 2272. <https://doi.org/10.3390/ani12172272>

Academic Editor: Marta Vascellari

Received: 15 June 2022

Accepted: 9 August 2022

Published: 2 September 2022

**Publisher's Note:** MDPI stays neutral with regard to jurisdictional claims in published maps and institutional affiliations.



**Copyright:** © 2022 by the authors. Licensee MDPI, Basel, Switzerland. This article is an open access article distributed under the terms and conditions of the Creative Commons Attribution (CC BY) license (<https://creativecommons.org/licenses/by/4.0/>).

**Keywords:** apoptosis; canine melanoma; cisplatin; inflammation; metastasis; para-toluenesulfonamide

## 1. Introduction

Melanoma, which develops from melanocytes, is a commonly occurring cancer in dogs [1]. These tumors exhibit an extremely variable biological behavior and are best characterized based on their site, size, stage, and histology [2]. Melanoma accounts for 3% of all neoplasms in dogs and up to 7% of all malignant tumors, and it is the most common oral malignancy (56%) [3]. The majority of oral melanomas in dogs exhibit malignant behavior, characterized by rapid invasion of surrounding normal tissues, metastasis to the regional lymph nodes and lungs, and occasionally metastasis to other distant organs [4]. In dogs with melanoma, especially in the oral cavity, the primary tumor size and distant metastasis and/or lymph node metastasis have been considered to be prognostic factors [5]. Chemotherapy has some effect in controlling distant metastasis of the tumor and may help improve the outcome after other initial treatments, such as surgery. Therefore, the most effective treatment should include chemotherapy in the adjuvant setting after surgery [6].

The PI3K/AKT/mTOR signaling pathway is a central pathway that promotes cell growth, cell motility, protein synthesis, survival, and metabolism in response to hormones, growth factors, and nutrients [7]. Recent research results have shown that, in human malignant melanoma, the RAF–MEK–ERK (MAPK) and PI3K–AKT–mTOR (AKT) signaling pathways are constitutively activated via multiple mechanisms [8,9]. The MAPK and AKT signal transduction pathways regulate cell survival, proliferation, and invasion, which are key functions in the progression of melanoma [7]. Downstream S6K1 is activated along with the PI3K/AKT/mTORC1 pathway, which in turn initiates a series of cellular responses related to tumor formation. Among these pathways are vascular proliferation and tumor-cell proliferation [10]. Thus, there is an interest in developing new therapeutic approaches that inhibit the mammalian target of rapamycin (mTOR) activation for treating tumors.

The small molecule para-toluenesulfonamide (PTS) has been shown *in vitro* and *in vivo* to display activity against human hepatocellular carcinoma, human nonsmall-cell lung cancer, and human tongue squamous cell carcinoma [11–13]. PTS is a therapeutic drug that is injected directly into the tumors and has been shown to induce cancer cell death by activating apoptosis and necrosis in a variety of cancers, with minimal damage to normal tissues [11,13]. Moreover, it has good lipophilicity, which enables it to easily enter tumors and become well distributed around them. Its mechanisms of action include damage to lysosomes by inducing the permeabilization of their membranes. This causes the release of cathepsin B and induces lysosome-mediated cell death [13]. Furthermore, PTS inhibited cell proliferation in human castration-resistant prostate cancer (CRPC) cell lines via the arrest of the cell cycle during the G1 phase, independent of p21 and p27 (a process that included the downregulation of cyclin D1 and the inhibition of the phosphorylation of the retinoblastoma protein) [14]. It also induced apoptosis by causing a substantial loss of membrane potential in the mitochondria. This loss of membrane potential likely resulted from the upregulation of the apoptosis regulators BAX and p53, which belong to the proapoptotic Bcl-2 family. This small molecule was also able to inhibit the phosphorylation of mTOR, 4EBP1, and p70S6K in CRPC cell lines. The inhibition of mTOR/p70S6K signaling in PC-3 cells was abrogated by overexpressing constitutively active Akt, revealing that this pathway is AKT-dependent. Overall, these findings (both *in vitro* and *in vivo*) suggest that PTS is an effective antitumor agent that acts by inhibiting the mTOR/p70S6K pathways, which are both AKT-dependent and AKT-independent [14].

Cisplatin is a broad-spectrum anticancer chemotherapeutic agent that is used in canine oral cancer treatment and has antitumor activity against oral malignant melanoma and squamous cell carcinomas in dogs in combination with the anti-inflammatory agent piroxicam or radiation therapy [1,15–17]. The efficacy of cisplatin depends on its ability to induce DNA damage because cisplatin is activated upon its entry into the cytoplasm

by displacing chloride atoms with water molecules, thus forming an electrophile with an affinity toward sulfhydryl groups on proteins and nitrogen donor atoms on nucleic acids [18]. Moreover, cisplatin, similar to many other chemotherapeutic drugs, can induce apoptosis; if the cells cannot repair the damage, they proceed to die [18–20]. The cellular toxicity of cisplatin results primarily from its ability to form intra- or interstrand crosslinks. The cells can become resistant through an enhanced ability to remove DNA adducts [21]. Cisplatin-based chemotherapy frequently results in acquired resistance via insufficient DNA binding, increased detoxification, increased DNA repair, deregulated expression of transporters, and altered expression and activation of genes involved in cell-death pathways, such as *p53*, *Bcl-2*, and *AKT/mTOR* [22]. Among these mechanisms, the activation of the *AKT/mTOR* pathway plays an important role in cisplatin resistance [23]. Boria et al. [1] treated oral melanomas with intravenous cisplatin (50–55 mg/m<sup>2</sup>) at 3-week intervals and with daily piroxicam (0.3 mg/kg), orally administered, and recorded an overall response rate of 18% and a median survival period of 119 days. In turn, Ahn et al. [24] reported that combination therapy of interferon beta and low-dose cisplatin significantly reduced canine melanoma tumor volume in a xenograft mouse model of canine melanoma. However, cisplatin resistance represents a problem for treatment, and other drugs are therefore often combined clinically with its application.

Here, we investigated the antitumor effects of the mTOR inhibitor PTS on melanoma cells. Furthermore, we examined its synergistic effects in combination with cisplatin. We implanted M5 canine melanoma cells in BALB/c nude mice and then assessed how tumor growth and aspects of cancer development (apoptosis, inflammation, and metastasis) were affected by these treatments.

## 2. Results

### 2.1. Tumor Growth Is Restricted by PTS

In the current study, treatment with both drugs (whether used individually or combined) led to smaller tumor size and volume relative to the control group (Figure 1a). Moreover, the time-course analysis showed that tumor growth was significantly retarded by all three treatments ( $p < 0.001$ ) relative to the control (Figure 1b). These effects were strongest when PTS and cisplatin were used together; cisplatin alone reduced tumor mass by 48.7%, PTS alone reduced it by 44.2%, and their combination reduced it by 72.8% relative to the control (Table 1). Thus, the growth of canine melanoma xenotransplants was extremely slowed in a mouse model after treatment with both PTS and cisplatin.

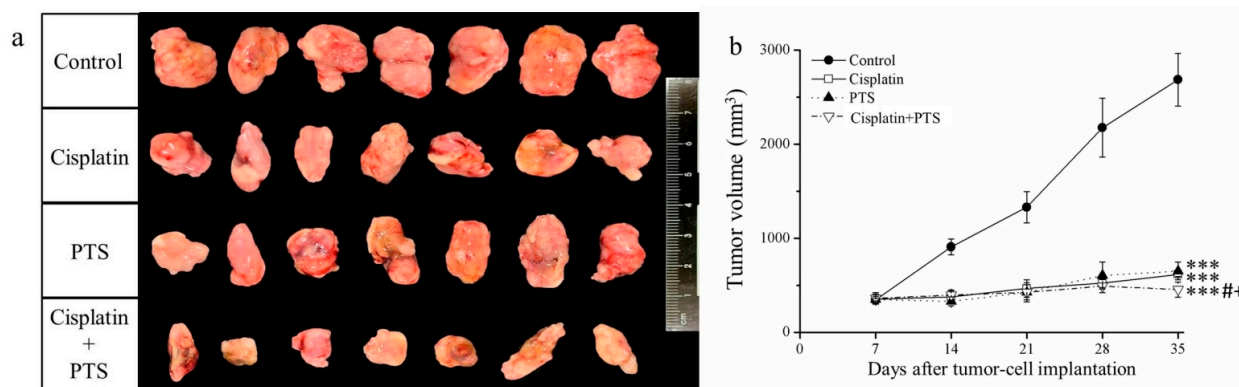


**Figure 1.** Effects of treatment with cisplatin, para-toluenesulfonamide (PTS), and their combination on M5 canine melanoma tumor growth in BALB/c nude mice. (a) Tumors excised from the mice 35 days after tumor-cell implantation. (b) Change in tumor volume over time. Treatments were administered from day 7 (when the tumors were detected) three times per week, as follows: saline (control), 2 mg/kg cisplatin (cisplatin), 100 mg/kg PTS (PTS), and 100 mg/kg PTS combined with 2 mg/kg cisplatin (cisplatin + PTS). Data are presented as mean  $\pm$  standard deviation (SD),  $n = 7$  per group. \*\*\*  $p < 0.001$  vs. control; #  $p < 0.05$  vs. cisplatin; +  $p < 0.05$  vs. PTS.

**Table 1.** Tumor masses after excision from sacrificed BALB/cByJNarl mice.

	Tumor Mass (g)	Tumor Mass Reduction (%)
Control	2.67 ± 0.32	–
Cisplatin	1.37 ± 0.25 ***	48.7
PTS	1.48 ± 0.33 ***	44.2
PTS + cisplatin	0.72 ± 0.19 ***#+	72.8

Data are presented as mean ± SD,  $n = 7$ . \*\*\*  $p < 0.001$  vs. control; #  $p < 0.05$  vs. cisplatin; +  $p < 0.05$  vs. PTS.

### 2.2. The Abundance of TUNEL-Positive Cells Increases in Response to PTS

An essential aspect of the growth and survival of all organisms is apoptosis, that is, programmed cell death. In the later stages of apoptosis, the DNA of dying cells becomes substantially degraded, and cells with this degraded DNA can be detected using a TUNEL assay [25]. Our TUNEL assay revealed that all three treatments resulted in an abundance of apoptotic cells. In the cisplatin group, the TUNEL-positive cell count was 3.9 times that of the control ( $p < 0.01$ ); in the PTS group, this ratio was 3.5 ( $p < 0.01$ ); and in the cisplatin + PTS group, it was 8.6 ( $p < 0.001$ ; Figure 2). The difference between the PTS and cisplatin groups was not significant, whereas that between the combined-treatment group and the other two treatment groups was significant ( $p < 0.001$ ). Thus, all three treatments enhanced apoptosis, but the combined treatment was by far the most effective of the three approaches in this respect.

### 2.3. The Expression of Apoptosis-Associated Proteins Is Affected by PTS Treatment

During the orchestrated process of apoptosis, specific enzymes are activated that dissolve the nuclear components of the apoptotic cells, including the protein components of both the nucleus and the cytoplasm [26]. To further assess the effects of our treatments on apoptosis, we analyzed several proteins with related functions: the antiapoptosis protein B-cell lymphoma 2 (Bcl-2), extracellular signal-regulated kinase (ERK), phosphorylated ERK, and cleaved caspase 3 (Figure 3a). According to our Western blotting analysis, cleaved caspase 3 and phosphorylated ERK were significantly upregulated in the cisplatin and PTS ( $p < 0.01$  for both) and cisplatin + PTS ( $p < 0.001$  for both) groups compared with the control group (Figure 3b,c). The combination-treatment group also exhibited the upregulation of these proteins versus both of the individual-treatment groups ( $p < 0.01$  for all except phosphorylated ERK in the cisplatin group, for which  $p < 0.05$ ). The expression of Bcl-2, which is thought to suppress apoptosis, was lower in the individual-treatment groups ( $p < 0.05$ ) and the combination-treatment group ( $p < 0.01$ ) than in the control group (Figure 3d). There was no significant difference in Bcl-2 expression between the PTS and cisplatin groups, whereas its expression in the cisplatin + PTS group was significantly lower than that detected in both individual-treatment groups ( $p < 0.05$  vs. PTS,  $p < 0.01$  vs. cisplatin). Thus, both the PTS and the cisplatin + PTS treatments enhanced the expression of proteins that are associated with the promotion of apoptosis and reduced the expression of a protein that inhibits apoptosis, although the combination treatment had the strongest effect.

### 2.4. The Production of Cytokines Is Restricted by PTS Administration

There are strong links between inflammation and cancer, and combating inflammation may improve the efficacy of cancer prevention and therapies [27]. One such approach consists in the suppression of the expression of inflammatory cytokines. We conducted an immunohistochemical (IHC) analysis of the histopathology of the tumors from our mice, focusing on the inflammatory cytokines of interleukin-1 $\beta$  (IL-1 $\beta$ ) (Figure 4a) and tumor necrosis factor- $\alpha$  (TNF- $\alpha$ ) (Figure 4b). The activity of both molecules was reduced in the cisplatin group by 29.7% and 77.4%, respectively; in the PTS group, it was reduced by 26.5% and 73.0%, respectively; and in the cisplatin + PTS group, it was reduced by 75.0% and 92.2%, respectively, relative to the control group (Figure 4c,d). There was no significant difference between the PTS and cisplatin groups regarding either cytokine, and the effect was once again strongest in the combination-treatment group. The reduction

in the cisplatin + PTS group relative to the PTS group was 65.9% for IL-1 $\beta$  and 71.3% for TNF- $\alpha$ , whereas relative to the cisplatin group, it was 64.4% for IL-1 $\beta$  and 65.8% for TNF- $\alpha$  ( $p < 0.01$  for all). This demonstrates that the combination treatment was able to strongly suppress the expression of these inflammatory cytokines in canine melanoma.

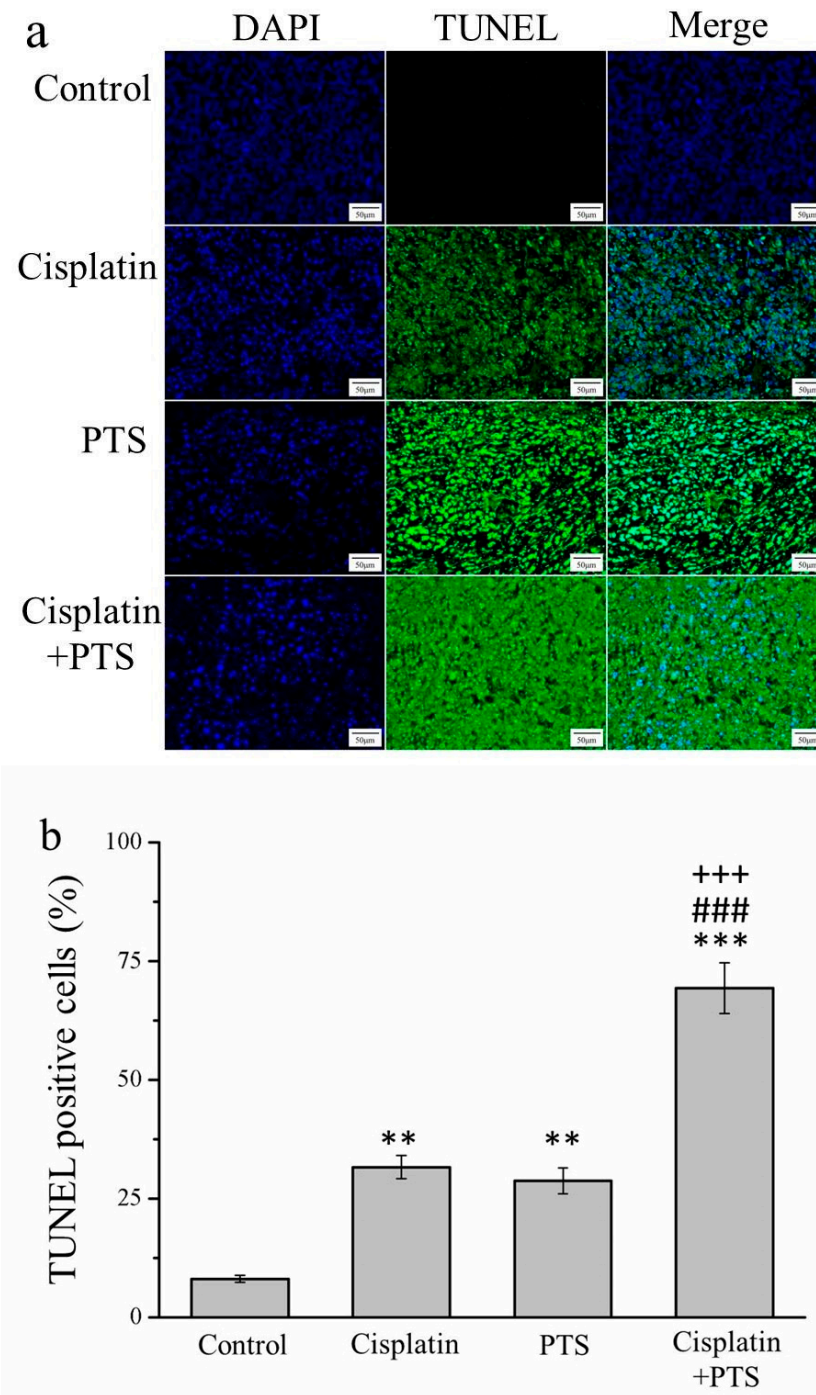


**Figure 2.** TUNEL/DAPI assay of apoptosis in M5 canine melanoma tumors implanted in BALB/c nude mice. (a) Staining with DAPI, TUNEL, and their merging. (b) Percentage of cells in the tumors that were TUNEL-positive in control mice and those administered with one of the following treatments three times per week, starting on day 7 (when the tumors were detected): saline (control), 2 mg/kg cisplatin (cisplatin), 100 mg/kg PTS (PTS), or 100 mg/kg PTS and 2 mg/kg cisplatin (cisplatin + PTS). Data are presented as mean  $\pm$  SD,  $n = 7$  per group. \*\*  $p < 0.01$ , \*\*\*  $p < 0.001$  vs. control; ###  $p < 0.001$  vs. cisplatin; +++  $p < 0.001$  vs. PTS. Scale bars: 50  $\mu$ m; magnification: 200 $\times$ .

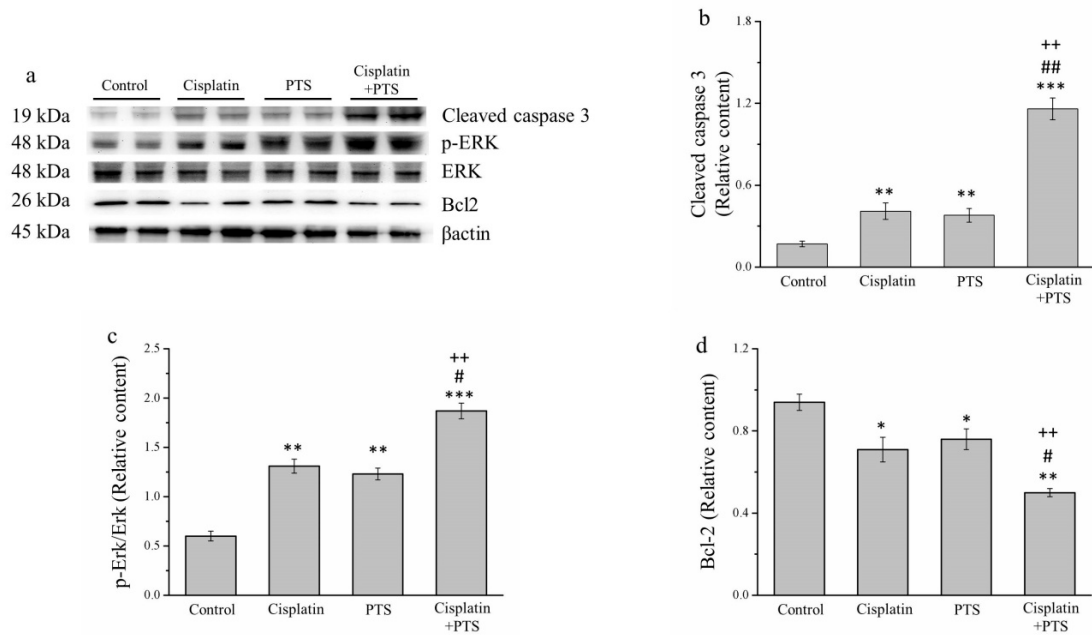


**Figure 3.** Western blot analysis of apoptosis-related proteins in M5 canine melanoma tumors implanted in BALB/c nude mice. (a) Representative Western blot. (b–d) Quantitative comparisons of the expression of cleaved caspase 3 (b), phosphorylated ERK (c), and (d) Bcl-2. The mice were administered the following treatments three times per week: saline (control), 2 mg/kg cisplatin (cisplatin), 100 mg/kg PTS (PTS), or 100 mg/kg PTS and 2 mg/kg cisplatin (cisplatin + PTS). Data are presented as mean ± SD, *n* = 7 per group. \* *p* < 0.05, \*\* *p* < 0.01, and \*\*\* *p* < 0.001 vs. control; # *p* < 0.05 and ## *p* < 0.01 vs. cisplatin; ++ *p* < 0.01 vs. PTS.

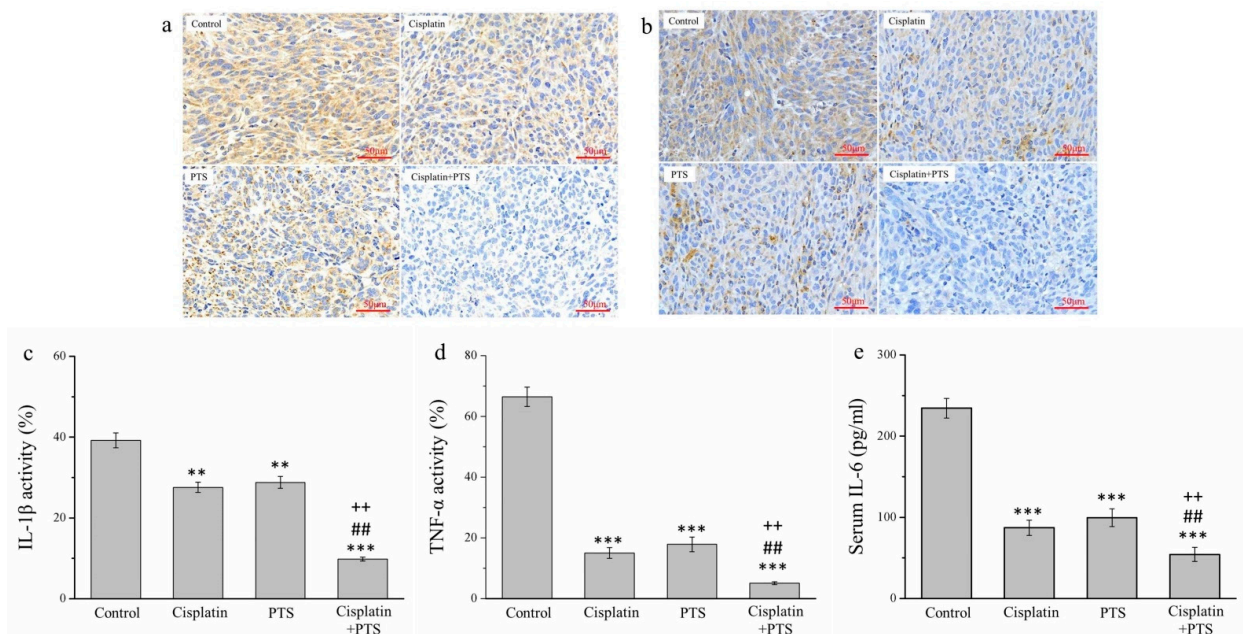


**Figure 4.** Immunohistochemical (IHC) analysis of the expression of three inflammatory cytokines in M5 canine melanoma tumors implanted in BALB/c nude mice. (a,b) Representative images showing IL-1β (a) and TNF-α (b) expression. (c–e) Quantitative analyses of the IHC expression of IL-1β (c), TNF-α (d), and serum IL-6 (e). The mice were administered the following treatments three times per week: saline (control), 2 mg/kg cisplatin (cisplatin), 100 mg/kg PTS (PTS), or 100 mg/kg PTS and 2 mg/kg cisplatin (cisplatin + PTS). Data are presented as mean ± SD, *n* = 7 per group. \*\* *p* < 0.01 and \*\*\* *p* < 0.001 vs. control; ## *p* < 0.01 vs. cisplatin; ++ *p* < 0.01 vs. PTS. Scale bars: 50 μm.

We also conducted an enzyme-linked immunosorbent assay to assess the serum expression of interleukin-6 (IL-6), which is another inflammatory cytokine. We observed a pattern similar to that of IL-1 $\beta$  and TNF- $\alpha$ . Relative to the control group, the expression of IL-6 in the cisplatin, PTS, and cisplatin + PTS groups was reduced by 62.8%, 57.5%, and 76.8%, respectively (Figure 4e). Here again, the difference between the cisplatin and PTS groups was not significant, but the levels in the combination-treatment group were significantly lower than those in both individual-treatment groups (by 37.6% and 45.4%, respectively;  $p < 0.01$  for both). Overall, these findings show that the administration of a combination of PTS and cisplatin strongly inhibited the expression of the inflammatory cytokines IL-1 $\beta$ , TNF- $\alpha$ , and IL-6 in canine melanoma.

### 2.5. The Expression of Inflammation-Related Factors Is Reduced in Response to PTS Administration

We conducted a Western blot analysis of factors related to inflammation. The expression of cyclooxygenase-2 (COX-2) in the cisplatin and PTS groups ( $p < 0.01$ ) and the combination-treatment group ( $p < 0.001$ ) was lower than that detected in the control group (Figure 5a). As described above, the difference between the cisplatin and PTS groups was not significant, whereas that between the combination-treatment group and the two individual-treatment groups was significant ( $p < 0.05$ ; Figure 5b).

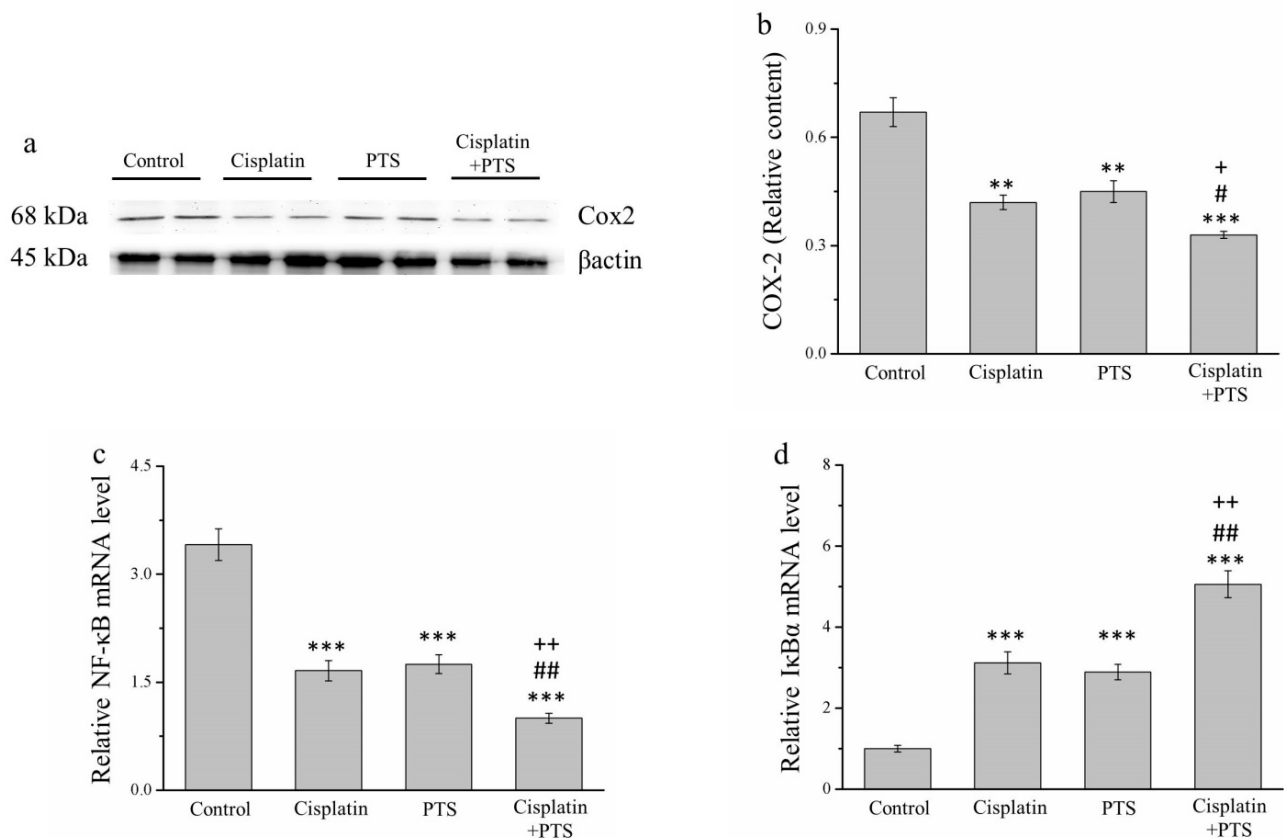


**Figure 5.** Analysis of factors related to inflammation in M5 canine melanoma tumors implanted in BALB/c nude mice. (a) Representative Western blot of cyclooxygenase-2 (COX-2). (b) Quantitative comparison of COX-2 expression in the four treatment groups. We conducted a quantitative polymerase chain reaction (PCR) to assess the relative mRNA expression levels of (c) *NF- $\kappa$ B* and (d) *I $\kappa$ B $\alpha$* . The mice were administered the following treatments three times per week: saline (control), 2 mg/kg cisplatin (cisplatin), 100 mg/kg PTS (PTS), or 100 mg/kg PTS and 2 mg/kg cisplatin (cisplatin + PTS). Data are presented as mean  $\pm$  SD,  $n = 7$  per group. \*\*  $p < 0.01$  and \*\*\*  $p < 0.001$  vs. control; #  $p < 0.05$  and ##  $p < 0.01$  vs. cisplatin; +  $p < 0.05$  and ++  $p < 0.01$  vs. PTS.

When cells are stimulated with inflammatory cytokines, I $\kappa$ B kinase (I $\kappa$ B $\alpha$ ) degrades them, leading to the inhibition of nuclear factor- $\kappa$ B (NF- $\kappa$ B), which then accumulates and regulates the expression of specific genes [28]. In our analysis of NF- $\kappa$ B and I $\kappa$ B $\alpha$  mRNA expression, we found that the expression of NF- $\kappa$ B was significantly lower in all three experimental groups ( $p < 0.001$  for all) than in the control group (Figure 5c). As expected, the reverse was true for I $\kappa$ B $\alpha$  expression ( $p < 0.001$  for all three experimental groups vs. control; Figure 5d). For both genes, there was no significant difference between the two individual-treatment groups, whereas the differences between each of them and the combination-treatment group were significant ( $p < 0.01$ ; Figure 5c,d). Overall, these findings indicate that PTS inhibited the expression of inflammation-related factors and responses, although this effect was not different from that of cisplatin. However, when the two agents were combined, the inhibition of the animals' inflammatory response was stronger.

### 2.6. Factors Related to Metastasis Are Reduced by PTS Administration

Metastasis is one of the primary reasons for the high morbidity and mortality associated with cancer and is thought to explain approximately 90% of cancer deaths [29]. Therefore, we analyzed the expression of transforming growth factor  $\beta$  (TGF- $\beta$ ), CD44, epidermal growth factor receptor (EGFR), and vascular endothelial growth factor (VEGF), all of which are related to metastasis. We analyzed TGF- $\beta$  and CD44 expression via IHC (Figure 6a,c) and that of EGFR and VEGF via Western blotting (Figure 6e). The expression of both TGF- $\beta$  and CD44 was reduced in the cisplatin and PTS groups ( $p < 0.01$  for all) and in the cisplatin + PTS group ( $p < 0.001$  for both) relative to the control group (Figure 6b,d). TGF- $\beta$  expression in the cisplatin, PTS, and cisplatin + PTS groups was reduced by 26.6%, 23.3%, and 62.6%, respectively, relative to the control group. Similarly, CD44 expression was reduced by 40.9%, 34.4%, and 61.6%, respectively. As reported above, the difference between the cisplatin and PTS groups was not significant, but significant differences were present between the combination-treatment group and the two individual-treatment groups ( $p < 0.01$  for all); expression in the cisplatin + PTS group was reduced by 49.0% and 51.2% (TGF- $\beta$ ) and 35.1% and 41.5% (CD44) relative to the cisplatin and PTS groups, respectively.

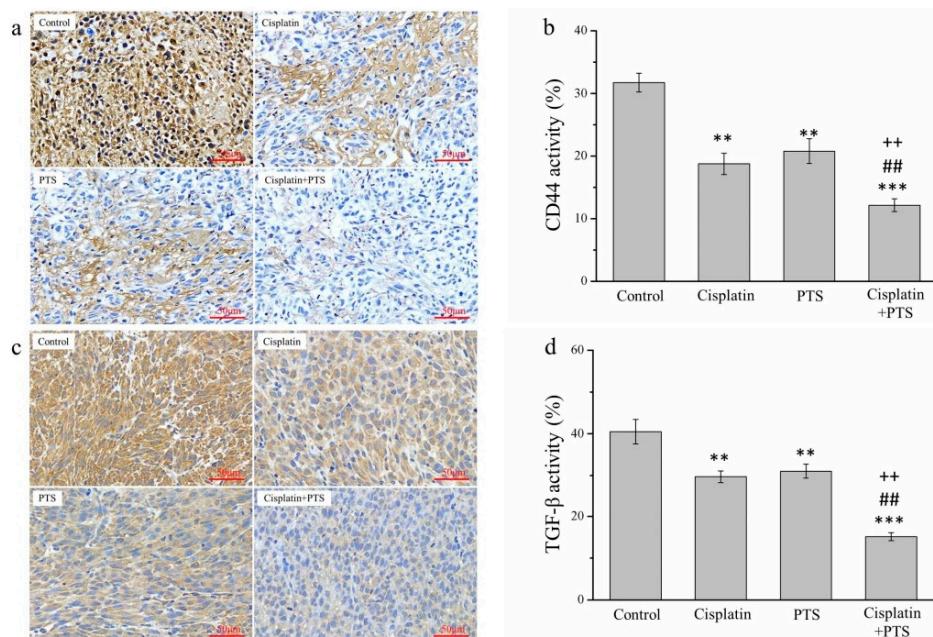
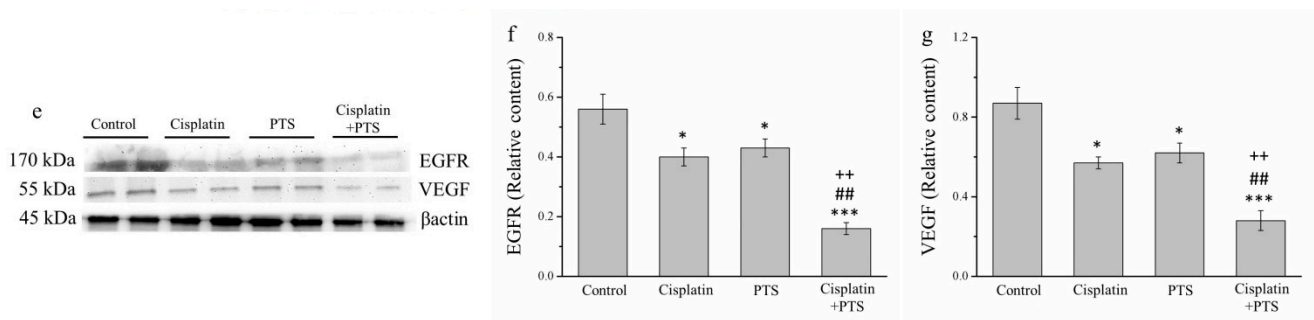


Figure 6. Cont.





**Figure 6.** Analysis of factors related to metastasis in M5 canine melanoma tumors implanted in BALB/c nude mice. (a–d) Representative images (a,c) and quantitative comparisons (b,d) from our IHC analysis of CD44 (a,b) and TGF- $\beta$  (c,d) expression. (e–g) Representative Western blot (e) from our analysis of the relative expression of EGFR (f) and VEGF (g). The mice were administered the following treatments three times per week: saline (control), 2 mg/kg cisplatin (cisplatin), 100 mg/kg PTS (PTS), or 100 mg/kg PTS and 2 mg/kg cisplatin (cisplatin + PTS). Data are presented as mean  $\pm$  SD,  $n = 7$  per group. \*  $p < 0.05$ , \*\*  $p < 0.01$ , and \*\*\*  $p < 0.001$  vs. control; ##  $p < 0.01$  vs. cisplatin; ++  $p < 0.01$  vs. PTS. Scale bars: 50  $\mu$ m.

The patterns of VEGF and EGFR expression were similar (Figure 6e). The expression of both of these factors was significantly lower in the individual-treatment groups ( $p < 0.05$  for all) and the combination-treatment group ( $p < 0.001$  for both) than in the control group (Figure 6f,g). Again, although there were no significant differences between the PTS and cisplatin groups, EGFR and VEGF expression in the cisplatin + PTS group was significantly lower than that detected in the remaining two treatment groups ( $p < 0.01$  for all). This shows that PTS treatment was able to inhibit the expression of these metastasis-related factors and that combining it with cisplatin augmented this effect.

### 3. Discussion

Here, we investigated the effects of treatment with PTS alone and in combination with cisplatin on M5 canine melanoma tumors implanted in nude mice. These mice have been used as an effective model for assessing the efficacy of treatments on ectopically xenotransplanted human carcinoma cells [30,31]. Tumor growth may be particularly favorable in such mice because they lack a thymus and, thus, cannot produce T cells [32]. We found that, similar to cisplatin, PTS treatment reduced tumor size and weight. Even though the effects of these two agents were similarly suppressive of tumors in all of our analyses, they achieved a substantially stronger antitumor effect when they were combined. Our findings indicated that this combination treatment promoted apoptosis by upregulating cleaved caspase 3 and phosphorylated ERK and downregulating Bcl-2. Furthermore, it reduced inflammation by restricting the production of IL-1 $\beta$ , TNF- $\alpha$ , IL-6, COX-2, and NF- $\kappa$ B. Finally, it rendered metastasis less likely by suppressing TGF- $\beta$ , CD44, VEGF, and EGFR.

The mTOR pathway is critical for regulating the cell cycle; it is an important downstream signaling pathway that is activated by many biological functions and plays a major role in regulating autophagy [33,34]. When this pathway is aberrantly activated, it produces signals that both promote tumor-cell growth and metastasis and enable these cells to invade healthy tissues [35]. Many clinical and histopathological similarities between human and canine melanoma were recognized by the Comparative Melanoma Tumor Board consensus study of the human relevance of melanoma in pet dogs [36]. Moreover, the study indicated that AKT and mTOR, as well as their downstream product, p70S6K, are present and active in canine melanoma cells. The activation of the mTOR pathway can be inhibited by rapamycin; in turn, the treatment of melanoma cells with rapamycin decreases the surviving tumor-cell fraction [37]. We were able to demonstrate that the inhibition of the mTOR pathway is an effective approach for treating cancer, and the research interest in inhibitors of this pathway has increased as a result. In the present study, we found that the

proliferation of M5 canine melanoma was restricted by PTS, suggesting that this approach may be useful in a clinical setting.

In human cancers, chemotherapy using a combination of an anticancer drug and a cell-signal inhibitor has been found in several studies to yield a better response than either drug in isolation. For example, combining rapamycin with sorafenib (a multikinase inhibitor that inhibits Raf-1 and B-RAF) synergistically reduces melanoma cell proliferation, and targeting these two types of signaling pathways simultaneously, may be more effective for treating melanoma than using either agent alone [38]. Research into drug combinations in canine melanoma treatment has also been conducted. The combination of the MEK inhibitor trametinib and the dual PI3K/mTOR inhibitor dactolisib synergistically decreased cell survival in association with caspase 3/7 activation and altered the expression of cell-cycle regulatory proteins and Bcl-2-family proteins [39]. Therefore, we assessed the inhibitory and synergistic effects of combining cisplatin with PTS to treat mice implanted with M5 canine melanoma cells. We found that, although PTS alone exhibited inhibitory effects, its combination with cisplatin strongly and synergistically inhibited tumor-cell growth. Alternatively, because of the small sample size of the mouse model, particularly serum volume, the toxic effects of PTS combined with cisplatin treatment were not estimated in this study. Previous reports indicated that the liver dysfunction induced by the intraperitoneal injection of a single dose of cisplatin (7.5 mg/kg body weight) on day 5 of the experiment was characterized by elevated serum levels of transaminases (aspartate aminotransferase (AST) and alanine transaminase (ALT)) [40,41]. In contrast, the serum ALT and AST levels were unaffected in rats treated with a single dose of 2 mg/kg of cisplatin [42]. Moreover, 4 years after the last PTS treatment, patients with hepatocellular carcinoma treated with PTS exhibited no abnormal liver function serum values [11]. To ensure that such liver damage is identified in a timely manner, clinicians should closely monitor the hepatic function of dogs with melanoma receiving PTS combined with cisplatin.

We then examined factors related to apoptosis. This is an important aspect of tumors because cancer cells are able to evade apoptosis despite having abnormalities and replicate themselves continuously. Chemotherapeutic approaches force the tumor cells to undergo apoptosis by causing cellular distress or DNA damage, in turn triggering cell-death signals [43]. We conducted TUNEL and DAPI assays to investigate the extent to which apoptosis occurred in the tumor cells in the mice. Similar to that observed for tumor growth, PTS on its own was beneficial as it enhanced tumor-cell apoptosis. However, in combination with cisplatin, the treatment strongly promoted apoptosis. Therefore, the latter treatment reduced the ability of tumor cells to evade apoptosis, thereby limiting tumor growth. We also observed the upregulation of cleaved caspase 3 and phosphorylated ERK, both of which are key for apoptosis, in mice treated with the combination regimen. Antiapoptotic Bcl-2 contributes to cancer formation and progression by promoting the survival of altered cells [44]. A previous study showed that an siRNA directed against the canine *Bcl-2* gene reduced Bcl-2 mRNA and protein expression in a canine malignant oral melanoma cell line (MCM-N1) and resulted in both a decrease in the number of viable cells and an increase in the apoptotic cell rate [45]. These findings indicate the important role of Bcl-2 activity in the inhibition of apoptosis in canine melanoma cells and reinforce the notion of Bcl-2 as a putative therapeutic target in tumors. We also found that PTS triggered the downregulation of *S6K1* and *mTOR* (Figure S1). As mentioned above, PTS must be able to suppress the expression of mTOR. In contrast, because the mTOR signaling pathway regulates autophagy and tumor-cell apoptosis, it can also promote tumor occurrence and progression. Sun et al. concluded that mTOR inhibits the expression of glycogen synthase kinase-3 (GSK-3) in prostate cancer cells. The downregulation of GSK-3, in turn, inhibits the caspase-3 signaling pathway, leading to the reduction in ROS production. Decreased ROS inhibit apoptosis in tumor cells to protect prostate cancer cells [46]. Accordingly, we found that PTS alone and combined with cisplatin triggered a significant upregulation of cleaved caspase 3 and phosphorylated ERK relative to the control group. This was probably caused by the inhibition of the mTOR pathway. Interestingly, in addition to its ability to induce

DNA damage, cisplatin induces tumor-cell apoptosis [18,19]. PTS combined with cisplatin enhanced the melanoma apoptosis afforded by the cisplatin alone treatment, as assessed by the IHC staining and Western blot analyses of apoptosis-related proteins performed in this study. Overall, these findings indicated that maximal antitumor effects were obtained when this PTS therapy was combined with a DNA-damaging chemotherapeutic agent. This study demonstrated the possible applicability of PTS for treating canine melanoma.

There is a well-established close link between chronic inflammation and tumor formation. Therefore, inflammation is thought to be a key characteristic of cancer [47]. In fact, various solid tumors maintain an inflammatory immune microenvironment, which enhances tumor development and metastasis [48]. Thus, we investigated the effects of PTS treatment on various factors related to inflammation (IL-1 $\beta$ , TNF- $\alpha$ , IL-6, COX-2, NF- $\kappa$ B, and I $\kappa$ B $\alpha$ ). The expression levels of the IL-1 $\beta$  gene or IL-1 $\beta$  protein are associated with the invasiveness and metastasis of melanoma [49]. Metastatic melanoma cell lines do not secrete IL-1 $\beta$ ; rather, they promote IL-1 $\beta$  production from macrophages in mice [50]. Moreover, a link between high levels of TNF- $\alpha$  and an increased risk of tumor formation and development has been described in vivo [51]. The effects of COX-2 in melanomas are thought to be largely caused by its role in the production of prostaglandins, especially prostaglandin E<sub>2</sub> [52]. Furthermore, in melanoma cells overexpressing COX-2, an increase in prostaglandin E<sub>2</sub> levels and expression of prostaglandin E<sub>2</sub> receptors resulted in the promotion of cell migration [53]. The transcription factor NF- $\kappa$ B regulates inflammatory responses by enhancing the expression of specific cellular genes, which is further linked to the promotion of carcinogenesis [54]. COX-2 is a major molecular target of NF- $\kappa$ B. Various inflammatory stimuli and mediators have been demonstrated to increase COX-2 expression via the activation of NF- $\kappa$ B, thus eliciting inflammation and consequent tumorigenesis [55,56]. In addition, IL-6, as one of the targets of NF- $\kappa$ B, can be regulated by STAT3 activation [57]. IL-6 was expressed in both human and dog melanomas. A previous study demonstrated that the prosurvival function of NF- $\kappa$ B was related to its functional interaction with the PI3K/AKT/mTOR signaling pathway [58]. With respect to factors that inhibit inflammation, the stimulation of TNF- $\alpha$  activates I $\kappa$ B, which is an important kinase that acts downstream in the TNF- $\alpha$  signaling pathway. It then phosphorylates I $\kappa$ B $\alpha$ , which causes its degradation by the ubiquitin–proteasome proteolytic system [59]. The susceptibility of malignant cells to apoptosis-inducing factors is increased by inhibiting NF- $\kappa$ B [60]. Therefore, NF- $\kappa$ B and I $\kappa$ B $\alpha$  play important roles in a range of inflammatory responses and immune processes. Here, the administration of PTS reduced the expression of IL-1 $\beta$ , TNF- $\alpha$ , IL-6, COX-2, NF- $\kappa$ B, and I $\kappa$ B $\alpha$ . Furthermore, C-reactive protein (CRP) is synthesized mainly as a result of stimulation by proinflammatory cytokines, and higher lung cancer risk and tumor progression are associated with elevated CRP levels [61]. Thus, it makes sense that the level of CRP was lowest in mice treated with both PTS and cisplatin (Figure S2).

The combination treatment also combated inflammation by suppressing inflammatory cytokines and promoting anti-inflammation mediators. This is another way in which PTS contributes to retarding tumor growth. In addition, the nuclear protein Ki67 is a marker of proliferation at inflamed sites and is strongly associated with tumor growth [62], to the extent that, in canine melanoma, the relative abundance of Ki67-positive tumor cells is used as a prognostic factor [63]. In fact, the Ki67 index differs significantly between malignant and benign melanocytic neoplasms in dogs and correlates negatively with survival [64]. We found that PTS, both alone and in combination with cisplatin, suppressed Ki67 expression (Figure S3). Overall, these findings showed that PTS effectively inhibited tumor-growth and antiapoptotic factors in canine melanoma cells by suppressing inflammation and tumor progression.

Metastasis is another key factor that determines cancer prognosis. The proliferation and migration of heavily transformed tumor cells are stimulated by TGF- $\beta$ , resulting in metastasis and tumor progression [65]. In canine oncology, little information is available regarding the association between anticancer immunity and the TGF- $\beta$  pathway. A previous

study found that the mean plasma TGF- $\beta$ 1 levels in tumor-bearing dogs were significantly higher than those in healthy controls [66]. Moreover, CD44 is a cell-surface molecule that mediates cell adhesion and communication with the extracellular matrix. In the case of melanoma, CD44 has been implicated in cell migration and proliferation in vitro [67,68]. CD44 is recognized as a cancer stem cell marker in canine breast tumors, and its expression is also increased in canine leukemia, melanoma, and osteosarcoma [69–72]. We found that PTS, used alone or in combination with cisplatin, substantially suppressed TGF- $\beta$  and CD44 expression, thereby reducing the metastatic potential of the tumor cells. It is also likely that the suppression of TGF- $\beta$  expression enhances the efficacy of drug therapy by helping to inhibit metastasis [73]. Furthermore, VEGF strongly promotes angiogenesis, and its overexpression is linked to tumor progression and metastasis [74]. Angiogenesis represents a fundamental step in the malignant growth of tumors and metastasis. Although many pro- and antiangiogenic factors affect the formation of new blood vessels, the central growth factor in this process is VEGF. Furthermore, VEGF expression appears to be related to tumor grade and prognosis in some malignancies [75]. Overexpression of VEGF in human melanoma results in a phenotype that has increased malignant potential compared with melanomas with low VEGF expression [76]. EGFR also has potential as an important therapeutic target in human cancer because it may be involved in the progression of cutaneous melanomas specifically [77] and more generally acts upstream of mTOR as a signal transducer of mitogens, which play a role in cancer pathogenesis and development [78]. In addition, the expression of the zinc finger E-box-binding homeobox 1 (ZEB1), a transcription factor that accelerates migration and invasion, indicates epithelial–mesenchymal transition (EMT) in canine melanoma cells [79]. Moreover, EMT-inducing ZEB1 promotes cancer cell metastasis and loss of cell polarity [80]. The aberrant expression of ZEB1 has been reported in a variety of human cancers, where it is generally believed to foster migration, invasion, and metastasis via mTOR signaling [81,82]. We found that treatment with PTS, both alone and in combination with cisplatin, reduced the expression of the mTOR/S6K1 signaling pathway, resulting in the suppression of the expression of the ZEB1 mRNA (Figure S4), possibly leading to a reduction in the potential for the M5 canine melanoma cells to metastasize. Therefore, our findings suggest that PTS exerts antitumor effects through the suppression of VEGF and EGFR expression, especially when administered in combination with cisplatin.

The tumors of canine and human melanomas are generally resistant to chemotherapy and radiation therapy. In veterinary oncology, no standard of care for melanoma has been firmly established. The treatment of dogs with melanoma consists primarily of surgery, with the options of hypofractionated or definitive radiation therapy and platinum chemotherapy [1,83–85]. Multiple veterinary studies have investigated therapeutic approaches incorporating carboplatin, cisplatin, and melphalan but only achieved poor response rates and no improvements in survival time. This is particularly the case when chemotherapeutic drugs are tested as the sole treatment or as adjuvant therapy after surgery or radiation therapy [1,86–88]. The development and metastasis of tumors are closely related to the tumor microenvironment, which varies in structure and function [89]. The tumor microenvironment can affect tumor progression, prognosis, and the efficacy of immunotherapy, with tumor-infiltrating lymphocytes being reportedly central to these effects [90]. We performed IHC staining using CD45, a marker of these lymphocytes, and found that CD45 activity was 1.4, 1.3, and 1.8 times higher in the cisplatin, PTS, and cisplatin + PTS groups, respectively, than in the control group (Figure S5). This further confirmed that PTS plays a key role in inhibiting these canine melanomas, although this effect was strongest in combination with cisplatin. This combined therapy significantly inhibited the growth of M5 cells by promoting apoptosis, suppressing inflammation, and reducing the potential for metastasis.

Melanomas are malignant neoplasms originating from melanocytes. Canine melanoma xenograft mouse models have been valuable in elucidating the mechanisms of malignant transformation, disease progression, and drug resistance in cutaneous melanoma [91,92].

However, mouse models for noncutaneous melanomas are still lacking, and mice have constraints, such as limited population heterogeneity, tightly controlled environmental living conditions, and the difficulty of obtaining serial tissue samples [93]. Accordingly, although melanomas occur in most animal species, the dog is considered the best animal model for this disease [16]. Alternatively, the route of PTS administration via local intratumoral injection can reveal the therapeutic effects of canine melanoma in xenografted mice. Moreover, the intratumoral injection of PTS is a palliative treatment that aims to further improve the survival and quality of life of patients with advanced or recurrent carcinomas, patients with cancer with severe comorbidities, or patients with a poor performance status [94]. However, a few published studies have shown that the association between chemotherapy with other therapy routes may potentially slow local progression and/or improve overall survival in canine melanoma [16,95]. Thus, future studies should focus on the individualized antitumor effect of therapies, representing a potential and powerful strategy for the treatment of melanomas in dogs, such as the combination of PTS with radiation therapy or PTS with chemotherapy.

#### 4. Materials and Methods

##### 4.1. Animals and Cell Line

We obtained germ-free male 6-week-old BALB/cByJNarl mice for use in this study (National Laboratory Animal Breeding and Research Center, Taipei, Taiwan). We housed two mice in each cage and provided them with sterile food and water. The mice had ad libitum access to Laboratory Rodent Diet 5058 (Lab Diet; Purina Mills, St. Louis, MO, USA) and were allowed to acclimate for 1 week prior to the collection of baseline weekly body-weight and food-intake changes. The mice were maintained in microisolation cages on HEPA-filtered ventilated racks (Rungshin IVC Systems, Taichung, Taiwan) under germ-free conditions with constant temperature ( $22 \pm 2$  °C) and relative humidity ( $55 \pm 5\%$ ) and a 12:12 h light:dark cycle. The bedding of the cages consisted of autoclaved shredded wood chips (Tapvei Oy, Kaavi, Finland). The cages were equipped with a variety of sterile toys of different shapes: tunnels, tubes, and triangles (Young Li, Taipei, Taiwan). The Institutional Animal Care and Use Committee (IACUC) at the National Chiayi University (IACUC Approval No. 110003) reviewed and approved our study protocol; the procedures of which were in accordance with the Guidelines for the Care and Use of Laboratory Animals published by the Taiwanese Ministry of Health and Welfare.

We obtained the M5 canine melanoma cell line from the School of Veterinary Medicine at National Taiwan University [96]. We cultured the cells in a humidified atmosphere (95% air, 5% CO<sub>2</sub>) at 37 °C in 90% high-glucose Dulbecco's Modified Eagle's Medium supplemented with 5% fetal bovine serum, 50 IU/mL of penicillin, and 50 mg/mL of streptomycin (Gibco Laboratories, Grand Island, NY, USA). We routinely passaged the cells by removing the medium and overlaying the cell monolayer with 0.25% trypsin and 0.1% ethylenediaminetetraacetic acid.

##### 4.2. Inoculation and Treatment of Tumors

The experimental treatments were commenced after the implanted M5 cells had formed a detectable tumor mass, which was assessed on day 7 after implantation. Briefly, we anesthetized the mice via intraperitoneal injection with Zoletil 50 (10 mg/kg; Virbac Taiwan, Taipei, Taiwan) and then subcutaneously injected 100 µL of a cell suspension containing 10<sup>7</sup> viable M5 cells into a posterior leg. We assessed the development of the tumor lesions on day 7 and randomly divided the animals that showed a distinct tumor of 4–5 mm in diameter [97] into four groups (seven animals per group). The control group received saline, and the three treatment groups received their treatments three times per week. The cisplatin group received 2 mg/kg cisplatin (Sigma, St. Louis, MO, USA) via intraperitoneal injection. The PTS group was administered 100 mg/kg PTS (Gongwin Biopharm Holding, Taipei, Taiwan) through local intratumoral injection. Finally, the cisplatin + PTS group received 100 mg/kg PTS and 2 mg/kg cisplatin. The dosage of

cisplatin used here was based on studies investigating how this drug affects apoptosis, invasion, metastasis, angiogenesis, and the growth signal mechanisms in canine melanomas implanted in mice [24]. We based the PTS dosage on the dose that is generally used to treat lung cancer [12], and the route of PTS administration was according to that reported in various studies [12,13,94,98]. We assessed the growth of the tumors every 7 days by measuring their largest and smallest diameters and calculated their volume according to the following formula:  $V = 0.5 \times a \times b^2$ , where  $a$  and  $b$  are the largest and smallest diameters, respectively.

#### 4.3. Clinical Observations and Histopathological Analysis

We observed the mice daily for clinical signs, weighed them every 3 days, and, at 35 days after tumor-cell implantation, euthanized them with an overdose of anesthetic (1.2 mg/kg urethane, intraperitoneally; Sigma) combined with carbon dioxide. Immediately before sacrificing the mice, we collected blood under anesthesia for hematological assessment. After euthanizing the mice, we immediately excised the tumors. We divided the tumor specimens into two groups. We treated one group with 10% formalin and embedded the specimens in paraffin. We investigated these specimens by subjecting them to hematoxylin and eosin staining; terminal deoxyribonucleotidyl transferase (TdT)-mediated biotin-16-dUTP nick-end labeling (TUNEL assay, APO-BrdU TUNEL Assay Kit; BD Pharmingen, San Diego, CA, USA); and IHC for IL-1 $\beta$ , TNF- $\alpha$ , TGF- $\beta$ , and CD44, using primary antibodies against these factors (Merck, Billerica, MA, USA). We assessed protein expression via IHC with the TAlink mouse/rabbit polymer detection system produced by BioTnA (Kaohsiung, Taiwan). We used a high-resolution digital microscope (Moticam 2300; Motic Instruments, Richmond, BC, Canada) equipped with Motic Images Plus (version 2.0) to capture and analyze the images. Regarding the other group of tumor specimens, we first minced them coarsely, homogenized them, and then stored them in a freezer at  $-80$  °C. We later subjected them to Western blotting to analyze the expression of cleaved caspase 3, ERK, Bcl-2, COX-2, VEGF, and EGFR.

#### 4.4. Measurement of the Serum Levels of IL-6

We measured the serum levels of IL-6 in the blood samples using commercial mouse kits (ab213749 and ab100697; Abcam, Cambridge, MA, USA) according to the manufacturer's protocol. We added 50  $\mu$ L of samples to each of the wells in 96-well antibody-coated plates and then incubated these for 2 h at room temperature. We then loaded 50  $\mu$ L of the detector antibody solution into each well and incubated the plates for an additional 1 h at room temperature. Next, we added 50  $\mu$ L of HRP-streptavidin solution (ab210901; Abcam) to each well and once again incubated the plates for 1 h at room temperature. Finally, we added 100  $\mu$ L of tetramethylbenzidine substrate to each well and incubated the plates for another 10 min in the dark at room temperature. We stopped the reaction by adding 100  $\mu$ L of stop solution. We read the absorbance at a wavelength of 450 nm and expressed the results in pg/mL.

#### 4.5. RNA Extraction and Real-Time Quantitative Polymerase Chain Reaction

We used the TRI Reagent (Sigma) to extract the total RNA from the tumor tissues. We quantified the RNA concentrations based on absorbance at 260–280 and 230–260 nm using a Qubit fluorometer (Invitrogen, Carlsbad, CA, USA). We reverse transcribed 1  $\mu$ g of the RNA into cDNA using an iScript cDNA synthesis kit (Bio-Rad, Hercules, CA, USA) according to the manufacturer's instructions. We performed a real-time polymerase chain reaction (PCR) using the cDNA and iTaq universal SYBR Green supermix (Bio-Rad) according to the manufacturer's protocol. We quantified the mRNA expression levels of *NF- $\kappa$ B* and *I $\kappa$ B $\alpha$*  using the CFX Connect Real-Time PCR Detection System (Bio-Rad). We used the following settings for PCR: 40 cycles of 95 °C for 30 s; 95 °C for 15 s, 60 °C for 30 s; and a final 5 min at 72 °C. We used the following sequence primers for *NF- $\kappa$ B*, *I $\kappa$ B $\alpha$* , and  $\beta$ -actin: *NF- $\kappa$ B*: forward, 5'-ATGGCTTCTATGAGGCTGAG-3' and reverse, 5'-

GTGTTGTTGGTCTGGATGC-3'; *IκBα*: forward, 5'-GCCCTTGTCCTGTCCCTA-3' and reverse, 5'-GCAGAGTATTTCCCTTTGGTTGA-3'; and *β-actin*: forward, 5'-ACTGGAACG GTGAAGGTGACA-3' and reverse, 5'-ATGGCAAGGGACTTCCTGTAAC-3' [99,100]. We calculated the expression levels of the two target genes relative to the *β-actin* levels and expressed them using the  $2^{-\Delta\Delta Ct}$  method.

#### 4.6. Western Blotting

We performed Western blotting on the second group of tumor specimens according to protocols reported in previous studies [101,102]. We used antibodies against *β-actin*, Bcl-2, COX-2, VEGF, and EGFR (Sigma) and against cleaved caspase 3, phosphorylated ERK (threonine 202/tyrosine 204), and ERK (Cell Signaling Technology, Beverly, MA, USA). We employed enhanced chemiluminescence reagents (Thermo Scientific, Rockford, MA, USA) to assess immunoreactivity and UVP ChemStudio (Analytik Jena, Upland, CA, USA) to detect signals. We quantified protein expression and phosphorylation using ImageJ (National Institutes of Health, Bethesda, MA, USA).

#### 4.7. Statistical Analysis

We presented all of the data as mean  $\pm$  standard deviation. We used *t*-tests to test for significant differences between pairs of groups. When comparing more than two groups, we performed an analysis of variance with a post-hoc Bonferroni correction. *p*-values below 0.05, 0.01, and 0.001 were considered significant, very significant, and extremely significant, respectively.

### 5. Conclusions

In conclusion, this study highlighted the co-effect of PTS and cisplatin for the potential treatment of canine melanoma. Our findings evidenced that PTS alone reduces the growth rate of canine melanoma xenotransplants in mice and that combining PTS with a traditional chemotherapy drug such as cisplatin yields a stronger inhibitory effect. This observation was associated with the inhibition of tumor growth via an apoptotic mechanism in canine melanoma cells, where the apoptotic expression of cleaved caspase 3 and ERK phosphorylation was enhanced, and the antiapoptotic expression of Bcl-2 was reduced. Furthermore, we found that PTS, both alone and combined with cisplatin, suppressed inflammatory cytokine (IL-1 $\beta$ , TNF- $\alpha$ , and IL-6) production, which may have retarded tumorigenesis. Treatments that have antitumor and anti-inflammatory effects result in lower levels of COX-2 and the *NF- $\kappa$ B* mRNA and higher levels of the *IκBα* mRNA. The inhibitory effect of PTS on the in-tumor mTOR pathway resulted in the downregulation of TGF- $\beta$ , CD44, VEGF, and EGFR, which would have had the effect of retarding tumor-cell migration and invasion, thus reducing the potential risk of metastasis. Overall, our in vivo findings regarding these xenograft-induced tumors in nude mice showed that PTS had a range of pharmacological effects in this experiment; it promoted apoptosis, suppressed inflammation, and supported mechanisms that suppress tumor metastasis. Moreover, combining cisplatin with PTS resulted in a stronger effect than using PTS alone. These findings suggest an avenue for investigating and developing additional therapeutic approaches for the treatment of canine melanoma specifically and cancers in general.

**Supplementary Materials:** The following supporting information can be downloaded at: <https://www.mdpi.com/article/10.3390/ani12172272/s1>. **Figure S1.** Western blot analysis of aspects of the mTOR signaling pathway in M5 canine melanoma tumors implanted in BALB/c nude mice. (a) Representative Western blot of mTOR and S6K1 expression. (b, c) Quantification of the relative expression levels of mTOR phosphorylation (b) and S6K1 phosphorylation (c). The mice were administered the following treatments three times per week: saline (control), 2 mg/kg cisplatin (cisplatin), 100 mg/kg PTS (PTS), or 100 mg/kg PTS and 2 mg/kg cisplatin (cisplatin + PTS). Data are presented as mean  $\pm$  SD, *n* = 7 per group. \* *p* < 0.05, \*\* *p* < 0.01, and \*\*\* *p* < 0.001 vs. control; # *p* < 0.05 vs. cisplatin; + *p* < 0.05 vs. PTS. **Figure S2.** Serum levels of CRP in BALB/cByJNarl mice implanted with canine melanoma tumor cells. The mice were administered the following treatments three

times per week: saline (control), 2 mg/kg cisplatin (cisplatin), 100 mg/kg PTS (PTS), or 100 mg/kg PTS and 2 mg/kg cisplatin (cisplatin + PTS). Data are presented as mean  $\pm$  SD,  $n = 7$  per group. \*\*\*  $p < 0.001$  vs. control; #  $p < 0.05$  vs. cisplatin; +  $p < 0.05$  vs. PTS. **Figure S3.** IHC analysis of Ki67 expression in M5 canine melanoma tumors implanted in BALB/c nude mice. (a) Representative IHC images indicating Ki67 expression. (b) Quantitative comparison of the expression levels of Ki67. The mice were administered the following treatments three times per week: saline (control), 2 mg/kg cisplatin (cisplatin), 100 mg/kg PTS (PTS), or 100 mg/kg PTS and 2 mg/kg cisplatin (cisplatin + PTS). Data are presented as mean  $\pm$  SD,  $n = 7$  per group. \*  $p < 0.05$  and \*\*\*  $p < 0.001$  vs. control; ##  $p < 0.01$  vs. cisplatin; ++  $p < 0.01$  vs. PTS. Scale bars: 50  $\mu$ m. **Figure S4.** Quantitative PCR analysis of the relative expression levels of the *ZEB1* mRNA in M5 canine melanoma tumors implanted in BALB/c nude mice. The mice were administered the following treatments three times per week: saline (control), 2 mg/kg cisplatin (cisplatin), 100 mg/kg PTS (PTS), or 100 mg/kg PTS and 2 mg/kg cisplatin (cisplatin + PTS). Data are presented as mean  $\pm$  SD,  $n = 7$  per group. \*\*\*  $p < 0.001$  vs. control; ##  $p < 0.01$  vs. cisplatin; ++  $p < 0.01$  vs. PTS. **Figure S5.** IHC analysis of CD45 expression in M5 canine melanoma tumors implanted in BALB/c nude mice. (a) Representative IHC images indicating Ki67 expression. (b) Quantitative comparison of the expression levels of Ki67. The mice were administered the following treatments three times per week: saline (control), 2 mg/kg cisplatin (cisplatin), 100 mg/kg PTS (PTS), or 100 mg/kg PTS and 2 mg/kg cisplatin (cisplatin + PTS). Data are presented as mean  $\pm$  SD,  $n = 7$  per group. \*  $p < 0.05$  and \*\*  $p < 0.01$  vs. control; #  $p < 0.05$  vs. cisplatin; +  $p < 0.05$  vs. PTS. Scale bars: 50  $\mu$ m. Serum CRP levels were measured using the mouse enzyme-linked immunosorbent assay kit (SEK50409; Sino Biological, Beijing, China). The *ZEB1* sequence primers employed in this study were as follows: forward, 5'-CCCTTGAAAGTGATCCAGCCA-3' and reverse, 5'-AGACCCAGAGTGTGAGAAGCG-3' [103]. The expression levels of each target gene were calculated relative to the  *$\beta$ -actin* levels and expressed using the  $2^{-\Delta\Delta C_t}$  method. To perform IHC staining for Ki67 and CD45 within the tumor samples, we obtained primary antibodies from Merck (Billerica, MA, USA). Moreover, the IHC-based expression levels were detected on a TALink mouse/rabbit polymer detection system from BioTnA (Kaohsiung, Taiwan).

**Author Contributions:** C.-T.L. conceived the idea and performed experiments. C.-F.L., J.-T.W., H.-P.T. and S.-Y.C. assisted in recombinant construction. H.-J.L., T.-C.L., C.-H.W. and Y.-C.L. analyzed the data. J.-H.W. and G.-R.C. wrote, reviewed, and edited the manuscript. All authors have read and agreed to the published version of the manuscript.

**Funding:** This study was supported in part by the National Chiayi University (Taiwan; 110A3-038 and 110A3-113).

**Institutional Review Board Statement:** The review of our experimental protocol was conducted by National Chiayi University's Institutional Animal Care and Use Committee, who approved it under the approval No. 110003.

**Informed Consent Statement:** Not applicable.

**Data Availability Statement:** The data presented in this study are available on request from the corresponding author.

**Acknowledgments:** The authors would like to thank LiTzung Biotechnology, Kaohsiung, Taiwan, for providing pathological assistance for this study.

**Conflicts of Interest:** The authors declare no conflict of interest.

## Abbreviations

PTS	Para-toluenesulfonamide
mTOR	Mammalian target of rapamycin
CRPC	Castration-resistant prostate cancer
IFN- $\beta$	interferon beta
COX-2	Cyclooxygenase-2
Bcl-2	B-cell lymphoma 2
VEGF	Vascular endothelial growth factor
EGFR	Epidermal growth factor receptor



ERK	Extracellular signal-related kinase
IL-1 $\beta$	Interleukin-1 $\beta$
IL-6	Interleukin-6
TNF- $\alpha$	Tumor necrosis factor- $\alpha$
CRP	C-reactive protein
I $\kappa$ B $\alpha$	I $\kappa$ B kinase
NF- $\kappa$ B	Nuclear factor $\kappa$ B
ZEB1	Zinc finger E-box-binding homeobox 1
IHC	Immunohistochemical
SD	Standard deviation

## References

- Boria, P.A.; Murry, D.J.; Bennett, P.F.; Glickman, N.W.; Snyder, P.W.; Merkel, B.L.; Schlittler, D.L.; Mutsaers, A.J.; Thomas, R.M.; Knapp, D.W. Evaluation of cisplatin combined with piroxicam for the treatment of oral malignant melanoma and oral squamous cell carcinoma in dogs. *J. Am. Vet. Med. Assoc.* **2004**, *224*, 388–394. [[CrossRef](#)] [[PubMed](#)]
- Bergman, P.J.; Kent, M.S.; Farese, J.P. Melanoma. In *Withrow and MacEwen's Small Animal Clinical Oncology*; Withrow, S., Vail, D., Page, R., Eds.; Elsevier Saunders: St. Louis, MO, USA, 2013; pp. 321–333.
- Almela, R.M.; Ansón, A. A Review of Immunotherapeutic Strategies in Canine Malignant Melanoma. *Vet. Sci.* **2019**, *6*, 15–27.
- Veena, P.; Kokila, S.; Rayadurgam, V.; Kumar, S.; Sankar, P.; Dhanalakshmi, N. Malignant melanoma in a Dog—A Case report. *Vet. World* **2012**, *5*, 431–432. [[CrossRef](#)]
- Atherton, M.J.; Morris, J.S.; McDermott, M.R.; Lichty, B.D. Cancer immunology and canine malignant melanoma: A comparative review. *Vet. Immunol. Immunopathol.* **2016**, *169*, 15–26. [[PubMed](#)]
- Ahn, H.J.; Na, I.I.; Park, Y.H.; Cho, S.Y.; Lee, B.C.; Koh, J.S.; Lee, Y.S.; Shim, Y.S.; Kim, Y.K.; Kang, H.J.; et al. Role of adjuvant chemotherapy in malignant mucosal melanoma of the head and neck. *Oral. Oncol.* **2010**, *46*, 607–611. [[CrossRef](#)]
- Sinnberg, T.; Lasithiotakis, L.; Niessner, H.; Schitteck, B.; Flaherty, K.T.; Kulms, D.; Maczey, E.; Campos, M.; Gogel, J.; Garbe, C.; et al. Inhibition of PI3K-AKT-mTOR Signaling Sensitizes Melanoma Cells to Cisplatin and Temozolomide. *J. Investig. Dermatol.* **2009**, *129*, 1500–1515. [[PubMed](#)]
- Keiran, S.M. A pivotal role for ERK in the oncogenic behaviour of malignant melanoma? *Int. J. Cancer* **2003**, *104*, 527–532.
- Xie, X.; White, E.P.; Mehnert, J.M. Coordinate Autophagy and mTOR Pathway Inhibition Enhances Cell Death in Melanoma. *PLoS ONE* **2013**, *8*, e55096.
- Kong, Y.; Si, L.; Li, Y.; Wu, X.; Xu, X.; Dai, J.; Tang, H.; Ma, M.; Chi, Z.; Sheng, X.; et al. Analysis of mTOR Gene Aberrations in Melanoma Patients and Evaluation of Their Sensitivity to PI3K-AKT-mTOR Pathway Inhibitors. *Clin. Cancer Res.* **2016**, *22*, 1018–1027.
- He, Q.; Kuang, A.R.; Guan, Y.S.; Liu, Y.Q. Puncture injection of para-toluenesulfonamide combined with chemoembolization for advanced hepatocellular carcinoma. *World J. Gastroenterol.* **2012**, *18*, 6861–6864. [[CrossRef](#)]
- Gao, Y.; Gao, Y.; Guan, W.; Huang, L.; Xu, X.; Zhang, C.; Chen, X.; Wu, Y.; Zeng, G.; Zhong, N. Antitumor effect of para-toluenesulfonamide against lung cancer xenograft in a mouse model. *J. Thorac. Dis.* **2013**, *5*, 472–483. [[PubMed](#)]
- Liu, Z.; Liang, C.; Zhang, Z.; Pan, J.; Xia, H.; Zhong, N.; Li, L. Para-toluenesulfonamide induces tongue squamous cell carcinoma cell death through disturbing lysosomal stability. *Anticancer Drugs* **2015**, *26*, 1026–1033. [[CrossRef](#)] [[PubMed](#)]
- Hsu, J.L.; Leu, W.J.; Hsu, L.C.; Liu, S.P.; Zhong, N.S.; Guh, J.H. Para-Toluenesulfonamide Induces Anti-tumor Activity Through Akt-Dependent and -Independent mTOR/p70S6K Pathway: Roles of Lipid Raft and Cholesterol Contents. *Front. Pharmacol.* **2018**, *9*, 1223. [[CrossRef](#)]
- Pisamai, S.; Roytrakul, S.; Phaonakrop, N.; Jaresitthikunchai, J.; Suriyaphol, G. Proteomic analysis of canine oral tumor tissues using MALDI-TOF mass spectrometry and in-gel digestion coupled with mass spectrometry (GeLC MS/MS) approaches. *PLoS ONE* **2018**, *13*, e0200619. [[CrossRef](#)] [[PubMed](#)]
- Nishiya, A.T.; Massoco, C.O.; Felizzola, C.R.; Perlmann, E.; Batschinski, K.; Tedardi, M.V.; Garcia, J.S.; Mendonça, P.P.; Teixeira, T.F.; Zaidan Dagli, M.L. Comparative Aspects of Canine Melanoma. *Vet. Sci.* **2016**, *3*, 7. [[CrossRef](#)]
- Freeman, K.P.; Hahn, K.A.; Harris, F.D.; King, G.K. Treatment of dogs with oral melanoma by hypofractionated radiation therapy and platinum-based chemotherapy (1987–1997). *J. Vet. Intern. Med.* **2003**, *17*, 96–101.
- Tchounwou, P.B.; Dasari, S.; Noubissi, F.K.; Ray, P.; Kumar, S. Advances in our understanding of the molecular mechanisms of action of cisplatin in cancer therapy. *J. Exp. Pharmacol.* **2021**, *13*, 303–328. [[CrossRef](#)]
- Seaman, F.; Sawhney, P.; Giammona, C.J.; Richburg, J.H. Cisplatin-induced pulse of germ cell apoptosis precedes long-term elevated apoptotic rates in C57/BL/6 mouse testis. *Apoptosis* **2003**, *8*, 101–108. [[CrossRef](#)]
- Plaimee, P.; Weerapreeyakul, N.; Barusrux, S.; Johns, N.P. Melatonin potentiates cisplatin-induced apoptosis and cell cycle arrest in human lung adenocarcinoma cells. *Cell Prolif.* **2015**, *48*, 67–77. [[CrossRef](#)]
- Bowden, N.A.; Ashton, K.A.; Kiejda, K.A.; Zhang, X.D.; Hersey, P.; Scott, R.J. Nucleotide Excision Repair Gene Expression after Cisplatin Treatment in Melanoma. *Cancer Res.* **2010**, *70*, 7918–7926. [[CrossRef](#)]
- Li, W.; Melton, D.W. Cisplatin regulates the MAPK kinase pathway to induce increased expression of DNA repair gene ERCC1 and increase melanoma chemoresistance. *Oncogene* **2012**, *31*, 2412–2422. [[CrossRef](#)] [[PubMed](#)]

23. Peng, D.J.; Wang, J.; Zhou, J.Y.; Wu, G.S. Role of the Akt/mTOR survival pathway in cisplatin resistance in ovarian cancer cells. *Biochem. Biophys. Res. Commun.* **2010**, *349*, 600–605. [[CrossRef](#)] [[PubMed](#)]
24. Ahn, J.O.; Lee, H.W.; Seo, K.W.; Kang, S.K.; Ra, J.C.; Youn, H.Y. Anti-Tumor Effect of Adipose Tissue Derived-Mesenchymal Stem Cells Expressing Interferon- $\beta$  and Treatment with Cisplatin in a Xenograft Mouse Model for Canine Melanoma. *PLoS ONE* **2013**, *8*, e74897.
25. Kyrylkova, K.; Kyryachenko, S.; Leid, M.; Kiouss, C. Detection of apoptosis by TUNEL assay. *Methods Mol. Biol.* **2012**, *887*, 41–47. [[PubMed](#)]
26. Sankari, S.L.; Masthan, K.M.; Babu, N.A.; Bhattacharjee, T.; Elumalai, M. Apoptosis in cancer—An update. *Asian Pac. J. Cancer Prev.* **2012**, *13*, 4873–4878. [[CrossRef](#)] [[PubMed](#)]
27. Desai, S.J.; Prickril, B.; Rasooly, A. Mechanisms of phytonutrient modulation of cyclooxygenase-2 (COX-2) and inflammation related to cancer. *Nutr. Cancer* **2018**, *70*, 350–375. [[CrossRef](#)]
28. Liu, T.; Zhang, L.; Joo, D.; Sun, S.C. NF- $\kappa$ B signaling in inflammation. *Signal Transduct. Target. Ther.* **2017**, *2*, 17203. [[CrossRef](#)]
29. Guan, X. Cancer metastases: Challenges and opportunities. *Acta. Pharm. Sin. B* **2015**, *5*, 402–418. [[CrossRef](#)]
30. Hseu, Y.C.; Chiang, Y.C.; Gowrisankar, Y.V.; Lin, K.Y.; Huang, S.T.; Shrestha, S.; Chang, G.R.; Yang, H.L. The in vitro and in vivo anticancer properties of chalcone flavokawain b through induction of ros-mediated apoptotic and autophagic cell death in human melanoma cells. *Cancers* **2020**, *12*, 2936. [[CrossRef](#)]
31. Souza, D.M.; Matheus, L.H.G.; Silva, C.S.; Ferreira, J.M.; Dellê, H. Renal Subcapsular Space of Balb/c Nude Mice as a Route for Evaluating Subpopulations of Human Bladder Carcinoma Cells. *In Vivo* **2016**, *30*, 383–386.
32. Tian, F.; Zhang, K.; Zheng, Z. Application of immunodeficiency rats and mice and analysis of common problems in oncology research. *Chin. J. Immunol.* **2016**, *2*, 214–217.
33. Davis, N.M.; Sokolosky, M.; Stadelman, K.; Abrams, S.L.; Libra, M.; Candido, S.; McCubrey, J.A. Deregulation of the EGFR/PI3K/PTEN/Akt/mTORC1 pathway in breast cancer: Possibilities for therapeutic intervention. *Oncotarget* **2014**, *5*, 4603–4650. [[CrossRef](#)]
34. Heras-Sandoval, D.; Pérez-Rojas, J.M.; Hernández-Damián, J.; Pedraza-Chaverri, J. The role of PI3K/AKT/mTOR pathway in the modulation of autophagy and the clearance of protein aggregates in neurodegeneration. *Cell. Signal.* **2014**, *26*, 2694–2701. [[CrossRef](#)] [[PubMed](#)]
35. Hsieh, A.C.; Liu, Y.; Edlind, M.P.; Ingolia, N.T.; Janes, M.R.; Sher, A.; Ruggero, D. The translational landscape of mTOR signalling steers cancer initiation and metastasis. *Nature* **2012**, *485*, 55–61. [[CrossRef](#)] [[PubMed](#)]
36. Simpson, R.M.; Bastian, B.C.; Michael, H.T.; Webster, J.D.; Prasad, M.L.; Conway, C.M.; Hewitt, S.M. Sporadic naturally occurring melanoma in dogs as a preclinical model for human melanoma. *Pigment Cell Melanoma Res.* **2014**, *27*, 37–47. [[CrossRef](#)] [[PubMed](#)]
37. Kent, M.S.; Collins, C.J.; Ye, F. Activation of the AKT and mammalian target of rapamycin pathways and the inhibitory effects of rapamycin on those pathways in canine malignant melanoma cell lines. *Am. J. Vet. Res.* **2009**, *70*, 263–269. [[CrossRef](#)] [[PubMed](#)]
38. Molhoek, K.R.; Brautigam, D.L.; Slingluff, C.L. Synergistic inhibition of human melanoma proliferation by combination treatment with B-Raf inhibitor BAY43-9006 and mTOR inhibitor Rapamycin. *J. Transl. Med.* **2005**, *3*, 39. [[CrossRef](#)] [[PubMed](#)]
39. Wei, B.R.; Michael, H.T.; Halsey, C.H.; Peer, C.J.; Adhikari, A.; Dwyer, J.E.; Simpson, R.M. Synergistic targeted inhibition of MEK and dual PI 3k/mTOR diminishes viability and inhibits tumor growth of canine melanoma underscoring its utility as a preclinical model for human mucosal melanoma. *Pigment Cell Melanoma Res.* **2016**, *29*, 643–655. [[CrossRef](#)]
40. dos Santos, N.A.; Martins, N.M.; Curti, C.; Pires Bianchi Mde, L.; dos Santos, A.C. Dimethylthiourea protects against mitochondrial oxidative damage induced by cisplatin in liver of rats. *Chem. Biol. Interact.* **2007**, *170*, 177–186. [[CrossRef](#)]
41. Boroja, T.; Katanić, J.; Rosić, G.; Selaković, D.; Joksimović, J.; Mišić, D.; Stanković, V.; Jovičić, N.; Mihailović, V. Summer savory (*Satureja hortensis* L.) extract: Phytochemical profile and modulation of cisplatin-induced liver, renal and testicular toxicity. *Food Chem. Toxicol.* **2018**, *118*, 252–263. [[CrossRef](#)]
42. Yonezawa, A.; Masuda, S.; Nishihara, K.; Yano, I.; Katsura, T.; Inui, K. Association between tubular toxicity of cisplatin and expression of organic cation transporter rOCT2 (Slc22a2) in the rat. *Biochem. Pharmacol.* **2005**, *70*, 1823–1831. [[CrossRef](#)] [[PubMed](#)]
43. Wong, R.S. Apoptosis in cancer: From pathogenesis to treatment. *J. Exp. Clin. Cancer Res.* **2011**, *30*, 87. [[CrossRef](#)] [[PubMed](#)]
44. Akl, H.; Vervloessem, T.; Kiviluoto, S.; Bittremieux, M.; Parys, J.B.; De Smedt, H.; Bultynck, G. A dual role for the anti-apoptotic Bcl-2 protein in cancer: Mitochondria versus endoplasmic reticulum. *Biochim. Biophys. Acta Mol. Cell Res.* **2014**, *1843*, 2240–2252.
45. Watanabe, Y.; Kano, R.; Maruyama, H.; Hasegawa, A.; Kamata, H. Small interfering RNA (siRNA) against the Bcl-2 gene increases apoptosis in a canine melanoma cell line. *J. Vet. Sci.* **2010**, *72*, 383–386. [[CrossRef](#)] [[PubMed](#)]
46. Sun, Y.; Ai, J.Z.; Jin, X.; Liu, L.R.; Lin, T.H.; Xu, H.; Yang, L. IL-8 protects prostate cancer cells from GSK-3 $\beta$ -induced oxidative stress by activating the mTOR signaling pathway. *Prostate* **2019**, *79*, 1180–1190. [[CrossRef](#)]
47. Punt, S.; Dronkers, E.A.; Welters, M.J.; Goedemans, R.; Koljenović, S.; Bloemena, E.; Jordanova, E.S. A beneficial tumor microenvironment in oropharyngeal squamous cell carcinoma is characterized by a high T cell and low IL-17+ cell frequency. *Cancer Immunol. Immunother.* **2016**, *65*, 393–403.
48. Beaugerie, L.; Itzkowitz, S.H. Cancers complicating inflammatory bowel disease. *N. Engl. J. Med.* **2015**, *372*, 1441–1452. [[CrossRef](#)]
49. Elaraj, D.M.; Weinreich, D.M.; Varghese, S.; Puhmann, M.; Hewitt, S.M.; Carroll, N.M.; Alexander, H.R. The role of interleukin 1 in growth and metastasis of human cancer xenografts. *Clin. Cancer Res.* **2006**, *12*, 1088–1096. [[CrossRef](#)]
50. Gehrke, S.; Otsuka, A.; Huber, R.; Meier, B.; Kistowska, M.; Fenini, G.; French, L.E. Metastatic melanoma cell lines do not secrete IL-1 $\beta$  but promote IL-1 $\beta$  production from macrophages. *J. Dermatol. Sci.* **2014**, *74*, 167–169. [[CrossRef](#)]

51. Lebrech, H.; Ponce, R.; Preston, B.D.; Iles, J.; Born, T.L.; Hooper, M. Tumor necrosis factor, tumor necrosis factor inhibition, and cancer risk. *Curr. Med. Res. Opin.* **2015**, *31*, 557–574. [[CrossRef](#)]
52. Wang, D.; DuBois, R.N. Eicosanoids and cancer. *Nat. Rev. Cancer* **2010**, *10*, 181–193. [[PubMed](#)]
53. Kim, K.M.; Im, A.R.; Kim, S.H.; Hyun, J.W.; Chae, S. Timosaponin AIII inhibits melanoma cell migration by suppressing COX-2 and in vivo tumor metastasis. *Cancer. Sci.* **2016**, *107*, 181–188. [[CrossRef](#)] [[PubMed](#)]
54. Kontos, S.; Sotiropoulou-Bonikou, G.; Kominea, A.; Melachrinou, M.; Balampani, E.; Bonikos, D. Coordinated increased expression of Cyclooxygenase2 and nuclear factor  $\kappa$ B is a steady feature of urinary bladder carcinogenesis. *Adv Urol.* **2010**, *2010*, 871356. [[CrossRef](#)] [[PubMed](#)]
55. Rakhesh, M.; Cate, M.; Vijay, R.; Shrikant, A.; Shanjana, A. A TLR4-interacting peptide inhibits lipopolysaccharide-stimulated inflammatory responses, migration and invasion of colon cancer SW480 cells. *Oncoimmunology* **2012**, *1*, 1495–1506. [[CrossRef](#)] [[PubMed](#)]
56. Wang, Y.; van Boxel-Dezaire, A.H.; Cheon, H.; Yang, J.; Stark, G.R. STAT3 activation in response to IL-6 is prolonged by the binding of IL-6 receptor to EGF receptor. *Proc. Natl. Acad. Sci. USA* **2013**, *110*, 16975–16980. [[CrossRef](#)] [[PubMed](#)]
57. Dan, H.C.; Cooper, M.J.; Cogswell, P.C.; Duncan, J.A.; Ting, J.P.Y.; Baldwin, A.S. Akt-dependent regulation of NF- $\kappa$ B is controlled by mTOR and Raptor in association with IKK. *Genes Dev.* **2008**, *22*, 1490–1500. [[CrossRef](#)]
58. Xia, L.; Tan, S.; Zhou, Y.; Lin, J.; Wang, H.; Oyang, L.; Liao, Q. Role of the NF $\kappa$ B-signaling pathway in cancer. *OncoTargets Ther.* **2018**, *11*, 2063–2073. [[CrossRef](#)]
59. Sakurai, H.; Suzuki, S.; Kawasaki, N.; Nakano, H.; Okazaki, T.; Chino, A.; Saiki, I. Tumor necrosis factor- $\alpha$ -induced IKK phosphorylation of NF- $\kappa$ B p65 on serine 536 is mediated through the TRAF2, TRAF5, and TAK1 signaling pathway. *J. Biol. Chem.* **2003**, *278*, 36916–36923. [[CrossRef](#)]
60. Karin, M.; Greten, F.R. NF- $\kappa$ B: Linking inflammation and immunity to cancer development and progression. *Nat. Rev. Immunol.* **2005**, *5*, 749–759.
61. Koch, A.; Fohlin, H.; Sörenson, S. Prognostic significance of C-reactive protein and smoking in patients with advanced non-small cell lung cancer treated with first-line palliative chemotherapy. *J. Thorac. Oncol.* **2009**, *4*, 326–332. [[CrossRef](#)] [[PubMed](#)]
62. Li, L.T.; Jiang, G.; Chen, Q.; Zheng, J.N. Ki67 is a promising molecular target in the diagnosis of cancer. *Mol. Med. Rep.* **2015**, *11*, 1566–1572.
63. Bergin, I.L.; Smedley, R.C.; Esplin, D.G.; Spangler, W.L.; Kiupel, M. Prognostic evaluation of Ki67 threshold value in canine oral melanoma. *Vet. Pathol.* **2011**, *48*, 41–53. [[PubMed](#)]
64. Smedley, R.C.; Spangler, W.L.; Esplin, D.G.; Kitchell, B.E.; Bergman, P.J.; Ho, H.Y.; Kiupel, M. Prognostic markers for canine melanocytic neoplasms: A comparative review of the literature and goals for future investigation. *Vet. Pathol.* **2011**, *48*, 54–72. [[PubMed](#)]
65. Massagué, J.; Blain, S.W.; Lo, R.S. TGF $\beta$  signaling in growth control, cancer, and heritable disorders. *Cell* **2000**, *103*, 295–309. [[PubMed](#)]
66. Itoh, H.; Horiuchi, Y.; Nagasaki, T.; Sakonju, I.; Kakuta, T.; Fukushima, U.; Takase, K. Evaluation of immunological status in tumor-bearing dogs. *Vet. Immunol. Immunopathol.* **2009**, *132*, 85–90.
67. Peck, D.; Isacke, C.M. CD44 phosphorylation regulates melanoma cell and fibroblast migration on, but not attachment to, a hyaluronan substratum. *Curr. Biol.* **1996**, *6*, 884–890.
68. Ahrens, T.; Sleeman, J.P.; Schempp, C.M.; Howells, N.; Hofmann, M.; Ponta, H.; Simon, J.C. Soluble CD44 inhibits melanoma tumor growth by blocking cell surface CD44 binding to hyaluronic acid. *Oncogene* **2001**, *20*, 3399–3408. [[PubMed](#)]
69. Zhou, B.; Jin, Y.; Zhang, D.; Lin, D. 5-Fluorouracil may enrich cancer stem cells in canine mammary tumor cells in vitro. *Oncol. Lett.* **2018**, *15*, 7987–7992. [[CrossRef](#)]
70. Gelain, M.E.; Martini, V.; Giantin, M.; Aricò, A.; Poggi, A.; Aresu, L.; Comazzi, S. CD44 in canine leukemia: Analysis of mRNA and protein expression in peripheral blood. *Vet. Immunol. Immunopathol.* **2014**, *159*, 91–96.
71. Guth, A.M.; Deogracias, M.; Dow, S.W. Comparison of cancer stem cell antigen expression by tumor cell lines and by tumor biopsies from dogs with melanoma and osteosarcoma. *Vet. Immunol. Immunopathol.* **2014**, *161*, 132–140.
72. Milovancev, M.; Hilgart-Martiszus, I.; McNamara, M.J.; Goodall, C.P.; Seguin, B.; Bracha, S.; Wickramasekara, S.I. Comparative analysis of the surface exposed proteome of two canine osteosarcoma cell lines and normal canine osteoblasts. *BMC Vet. Res.* **2013**, *9*, 116. [[CrossRef](#)] [[PubMed](#)]
73. Ciftci, K.; Su, J.; Trovitch, P.B. Growth factors and chemotherapeutic modulation of breast cancer cells. *J. Pharm. Pharmacol.* **2003**, *55*, 1135–1141. [[CrossRef](#)] [[PubMed](#)]
74. Citri, A.; Yarden, Y. EGF-ERBB signalling: Towards the systems level. *Nat. Rev. Mol. Cell Biol.* **2006**, *7*, 505–516.
75. Chaudhry, I.H.; O'donovan, D.G.; Brenchley, P.E.C.; Reid, H.; Roberts, I.S.D. Vascular endothelial growth factor expression correlates with tumour grade and vascularity in gliomas. *Histopathology* **2001**, *39*, 409–415. [[PubMed](#)]
76. Platt, S.R.; Scase, T.J.; Adams, V.; Wieczorek, L.; Miller, J.; Adamo, F.; Long, S. Vascular endothelial growth factor expression in canine intracranial meningiomas and association with patient survival. *J. Vet. Intern. Med.* **2006**, *20*, 663–668. [[CrossRef](#)]
77. Boone, B.; Jacobs, K.; Ferdinande, L.; Taildeman, J.; Lambert, J.; Peeters, M.; Brochez, L. EGFR in melanoma: Clinical significance and potential therapeutic target. *J. Cutan. Pathol.* **2011**, *38*, 492–502.
78. Baselga, J.; Arteaga, C.L. Critical update and emerging trends in epidermal growth factor receptor targeting in cancer. *J. Clin. Oncol.* **2005**, *23*, 2445–2459.

79. Veloso, E.S.; Gonçalves, I.N.N.; Silveira, T.L.; Santo, J.T.E.; Figueiredo, L.V.; Varaschin, M.S.; Ferreira, E. ZEB and Snail expression indicates epithelial-mesenchymal transition in canine melanoma. *Res. Vet. Sci.* **2020**, *131*, 7–14.
80. Krebs, A.M.; Mitschke, J.; Lasierra Losada, M.; Schmalhofer, O.; Boerries, M.; Busch, H.; Boettcher, M.; Mougiakakos, D.; Reichardt, W.; Bronsert, P.; et al. The EMT-activator Zeb1 is a key factor for cell plasticity and promotes metastasis in pancreatic cancer. *Nat. Cell Biol.* **2017**, *19*, 518–529.
81. Caramel, J.; Ligier, M.; Puisieux, A. Pleiotropic Roles for ZEB1 in Cancer. *Cancer Res.* **2018**, *78*, 30–35.
82. Chen, H.; Zhu, D.; Zheng, Z.; Cai, Y.; Chen, Z.; Xie, W. CEP55 promotes epithelial-mesenchymal transition in renal cell carcinoma through PI3K/AKT/mTOR pathway. *Clin. Transl. Oncol.* **2019**, *21*, 939–949. [[CrossRef](#)] [[PubMed](#)]
83. Bostock, D.E. Prognosis after surgical excision of canine melanomas. *Vet. Pathol.* **1979**, *16*, 32–40. [[CrossRef](#)] [[PubMed](#)]
84. Blackwood, L.; Dobson, J.M. Radiotherapy of oral malignant melanomas in dogs. *J. Am. Vet. Med. Assoc.* **1996**, *209*, 98–102. [[PubMed](#)]
85. Theon, A.P.; Rodriguez, C.; Madewell, B.R. Analysis of prognostic factors and patterns of failure in dogs with malignant oral tumors treated with megavoltage irradiation. *J. Am. Vet. Med. Assoc.* **1997**, *210*, 778–784. [[PubMed](#)]
86. Rassnick, K.M.; Ruslander, D.M.; Cotter, S.M.; Al-Sarraf, R.; Bruyette, D.S.; Gamblin, R.M.; Moore, A.S. Use of carboplatin for treatment of dogs with malignant melanoma: 27 cases (1989–2000). *J. Am. Vet. Med. Assoc.* **2001**, *218*, 1444–1448. [[CrossRef](#)]
87. Brockley, L.K.; Cooper, M.A.; Bennett, P.F. Malignant melanoma in 63 dogs (2001–2011): The effect of carboplatin chemotherapy on survival. *N. Z. Vet. J.* **2013**, *61*, 25–31. [[CrossRef](#)]
88. Murphy, S.; Hayes, A.M.; Blackwood, L.; Maglennon, G.; Pattinson, H.; Sparkes, A.H. Oral malignant melanoma—the effect of coarse fractionation radiotherapy alone or with adjuvant carboplatin therapy. *Vet. Comp. Oncol.* **2005**, *3*, 222–229. [[CrossRef](#)]
89. Yang, M.; Li, J.; Gu, P.; Fan, X. The application of nanoparticles in cancer immunotherapy: Targeting tumor microenvironment. *Bioact. Mater.* **2021**, *6*, 1973–1987. [[CrossRef](#)]
90. Geng, Y.; Shao, Y.; He, W.; Hu, W.; Xu, Y.; Chen, J.; Jiang, J. Prognostic role of tumor-infiltrating lymphocytes in lung cancer: A meta-analysis. *Cell. Physiol. Biochem.* **2015**, *37*, 1560–1571. [[CrossRef](#)]
91. van der Weyden, L.; Patton, E.E.; Wood, G.A.; Foote, A.K.; Brenn, T.; Arends, M.J.; Adams, D.J. Cross-species models of human melanoma. *J. Pathol.* **2016**, *238*, 152–165. [[CrossRef](#)]
92. Pérez-Guijarro, E.; Day, C.P.; Merlino, G.; Zaidi, M.R. Genetically engineered mouse models of melanoma. *Cancer* **2017**, *123* (Suppl. S11), 2089–2103. [[CrossRef](#)] [[PubMed](#)]
93. Hernandez, B.; Adissu, H.A.; Wei, B.R.; Michael, H.T.; Merlino, G.; Simpson, R.M. Naturally occurring canine melanoma as a predictive comparative oncology model for human mucosal and other triple wild-type melanomas. *Int. J. Mol. Sci.* **2018**, *19*, 394. [[CrossRef](#)] [[PubMed](#)]
94. Li, S.Y.; Li, Q.; Guan, W.J.; Huang, J.; Yang, H.P.; Wu, G.M.; Jin, F.G.; Hu, C.P.; Chen, L.A.; Xu, G.L.; et al. Effects of para-toluenesulfonamide intratumoral injection on non-small cell lung carcinoma with severe central airway obstruction: A multi-center, non-randomized, single-arm, open-label trial. *Lung Cancer* **2016**, *98*, 43–50. [[CrossRef](#)] [[PubMed](#)]
95. Cancedda, S.; Rohrer Bley, C.; Aresu, L.; Dacasto, M.; Leone, V.F.; Pizzoni, S.; Gracis, M.; Marconato, L. Efficacy and side effects of radiation therapy in comparison with radiation therapy and temozolomide in the treatment of measurable canine malignant melanoma. *Vet. Comp. Oncol.* **2016**, *14*, e146–e157. [[CrossRef](#)]
96. Liu, I.L.; Chung, T.F.; Huang, W.H.; Hsu, C.H.; Liu, C.C.; Chiu, Y.H.; Huang, K.C.; Liao, A.T.; Lin, C.S. Kynurenine 3-monooxygenase (KMO), and signal transducer and activator of transcription 3 (STAT3) expression is involved in tumour proliferation and predicts poor survival in canine melanoma. *Vet. Comp. Oncol.* **2021**, *19*, 79–91. [[CrossRef](#)]
97. Zhang, B.; Jin, K.; Jiang, T.; Wang, L.; Shen, S.; Luo, Z.; Pang, Z. Celecoxib normalizes the tumor microenvironment and enhances small nanotherapeutics delivery to A549 tumors in nude mice. *Sci. Rep.* **2017**, *7*, 10071. [[CrossRef](#)]
98. Guan, W.J.; Li, S.Y.; Zhong, N.S. Effects of para-toluenesulfonamide intratumoral injection on pulmonary adenoid cystic carcinoma complicating with severe central airway obstruction: A 5-year follow-up study. *J. Thorac. Dis.* **2018**, *10*, 2448–2455. [[CrossRef](#)]
99. Attafi, I.M.; Bakheet, S.A.; Korashy, H.M. The role of NF- $\kappa$ B and AhR transcription factors in lead-induced lung toxicity in human lung cancer A549 cells. *Toxicol. Mech. Methods.* **2020**, *30*, 197–207. [[CrossRef](#)]
100. Zeng, W.; Li, H.; Chen, Y.; Lv, H.; Liu, L.; Ran, J.; Li, H. Survivin activates NF- $\kappa$ B p65 via the IKK $\beta$  promoter in esophageal squamous cell carcinoma. *Mol. Med. Rep.* **2016**, *13*, 1869–1880. [[CrossRef](#)]
101. Wu, C.F.; Hou, P.H.; Mao, F.C.; Su, Y.C.; Wu, C.Y.; Yang, W.C.; Lin, C.S.; Tsai, H.P.; Liao, H.Y.; Chang, G.R. Mirtazapine reduces adipocyte hypertrophy and increases glucose transporter expression in obese mice. *Animals* **2020**, *10*, 1423. [[CrossRef](#)]
102. Tsai, H.P.; Hou, P.H.; Mao, F.C.; Chang, C.C.; Yang, W.C.; Wu, C.F.; Liao, H.J.; Lin, T.C.; Chou, L.S.; Hsiao, L.W.; et al. Risperidone exacerbates glucose intolerance, nonalcoholic fatty liver disease, and renal impairment in obese mice. *Int. J. Mol. Sci.* **2021**, *22*, 409. [[CrossRef](#)] [[PubMed](#)]
103. Giacomelli, C.; Daniele, S.; Romei, C.; Tavanti, L.; Neri, T.; Piano, I.; Trincavelli, M.L. The A2B adenosine receptor modulates the epithelial-mesenchymal transition through the balance of cAMP/PKA and MAPK/ERK pathway activation in human epithelial lung cells. *Front. Pharmacol.* **2018**, *9*, 54. [[CrossRef](#)] [[PubMed](#)]